

# eRD14 - EIC PID Consortium

- An integrated program for particle identification (PID) for a future Electron-Ion Collider (EIC) detector.

M. Alfred<sup>10</sup>, L. Allison<sup>18</sup>, M. Awadi<sup>10</sup>, B. Azmoun<sup>3</sup>, F. Barbosa<sup>13</sup>, M. Boer<sup>16</sup>, W. Brooks<sup>20</sup>, T. Cao<sup>24</sup>, M. Chiu<sup>3</sup>, E. Cisbani<sup>13,14</sup>, M. Contalbrigo<sup>12</sup>, S. Danagoulian<sup>17</sup>, A. Datta<sup>23</sup>, A. Del Dotto<sup>13</sup>, M. Demarteau<sup>2</sup>, A. Denisov<sup>11</sup>, J.M. Durham<sup>16</sup>, A. Durum<sup>11</sup>, R. Dzhygadlo<sup>9</sup>, D. Fields<sup>23</sup>, Y. Furlitova<sup>15</sup>, C. Gleason<sup>19</sup>, M. Grosse-Perdekamp<sup>22</sup>, J. Harris<sup>25</sup>, X. He<sup>8</sup>, H. van Hecke<sup>16</sup>, T. Horn<sup>4</sup>, J. Huang<sup>3</sup>, C. Hyde<sup>18</sup>, Y. Ilieva<sup>24</sup>, G. Kalicy<sup>4</sup>, A. Kebede<sup>17</sup>, B. Kim<sup>5</sup>, E. Kistenev<sup>3</sup>, Y. Kulinich<sup>22</sup>, M. Liu<sup>16</sup>, R. Majka<sup>30</sup>, J. McKisson<sup>15</sup>, R. Mendez<sup>20</sup>, P. Nadel-Turonski<sup>19</sup>, K. Park<sup>13</sup>, K. Peters<sup>9</sup>, T. Rao<sup>3</sup>, R. Pisani<sup>3</sup>, P. Rossi<sup>15</sup>, M. Sarsour<sup>8</sup>, C. Schwarz<sup>9</sup>, J. Schwiening<sup>9</sup>, C.L. da Silva<sup>16</sup>, N. Smirnov<sup>25</sup>, J. Stevens<sup>6</sup>, A. Sukhanov<sup>3</sup>, S. Syed<sup>8</sup>, J. Toh<sup>22</sup>, R. Towell<sup>1</sup>, T. Tsang<sup>3</sup>, G. Varner<sup>21</sup>, R. Wagner<sup>2</sup>, C. Woody<sup>3</sup>, C.-P. Wong<sup>8</sup>, W. Xi<sup>15</sup>, J. Xie<sup>2</sup>, Z.W. Zhao<sup>7</sup>, B. Zihlmann<sup>15</sup>, C. Zorn<sup>15</sup>.

Contacts: P. Nadel-Turonski <turonski@jlab.org>, Y. Ilieva <jordanka@physics.sc.edu>

<sup>1</sup>) Abilene Christian University, Abilene, TX 79601

<sup>2</sup>) Argonne National Lab, Argonne, IL 60439

<sup>3</sup>) Brookhaven National Lab, Upton, NY 11973

<sup>4</sup>) Catholic University of America, Washington, DC 20064

<sup>5</sup>) City College of New York, New York, NY 10031

<sup>6</sup>) College of William & Mary, Williamsburg, VA 2318

<sup>7</sup>) Duke University, Durham, NC 27708

<sup>8</sup>) Georgia State University, Atlanta, GA 30303

<sup>9</sup>) GSI Helmholtzzentrum für Schwerionenforschung GmbH, 64291 Darmstadt, Germany

<sup>10</sup>) Howard University, Washington, DC 20059

<sup>11</sup>) Institute for High Energy Physics, Protvino, Russia

<sup>12</sup>) INFN, Sezione di Ferrara, 44100 Ferrara, Italy

<sup>13</sup>) INFN, Sezione di Roma, 00185 Rome, Italy

<sup>14</sup>) Istituto Superiore di Sanità, 00161 Rome, Italy

<sup>15</sup>) Jefferson Lab, Newport News, VA 23606

<sup>16</sup>) Los Alamos National Lab, Los Alamos, NM 87545

<sup>17</sup>) North Carolina A&T State University, Greensboro, NC 27411

<sup>18</sup>) Old Dominion University, Norfolk, VA 23529

<sup>19</sup>) Stony Brook University, Stony Brook, NY 11794

<sup>20</sup>) Universidad Técnica Federico Santa María, Valparaíso, Chile

<sup>21</sup>) University of Hawaii, Honolulu, HI 96822

<sup>22</sup>) University of Illinois, Urbana-Champaign, IL 61801

<sup>23</sup>) University of New Mexico, Albuquerque, NM 87131

<sup>24</sup>) University of South Carolina, Columbia, SC 29208

<sup>25</sup>) Yale University, New Haven, CT 06520

# Table of Contents

<b>1. Introduction</b>	<b>3</b>
<b>2. Hadron identification</b>	<b>5</b>
2.1 PID requirements and implementation options	5
2.1.1 Hadron ID requirements	5
2.1.2 Integrated PID solution for the EIC (concept) detector(s)	6
2.2 Dual-radiator RICH (dRICH)	10
2.2.1 dRICH Simulation and Status	11
2.2.2 dRICH Prototype	13
2.2.3 FY17 Progresses and Achievements	14
2.2.4 Proposed dRICH R&D Activities	14
2.2.5 dRICH R&D Deliverables	15
2.3 Modular Aerogel RICH (mRICH)	15
2.3.2 Proposed mRICH R&D Activities	18
2.3.3 mRICH R&D Deliverables	18
2.4 DIRC	18
2.4.1 FY17: Progress and Achievements	20
Hardware: Development and Validation of the 3-layer Spherical Lens	20
2.4.2 Proposed DIRC R&D Activities	23
2.4.3 DIRC R&D Deliverables	25
2.5 High-resolution Time-of-Flight (TOF)	26
2.5.1 FY17 Progress and Achievements	26
2.5.2 Proposed TOF R&D Activities	28
2.5.3 TOF R&D Deliverables	30
<b>3. Lepton (electron) Identification</b>	<b>31</b>
3.1 Electron ID	31
3.2 Muon ID	33
<b>4. Photosensors &amp; Electronics</b>	<b>33</b>
4.1.1 FY17 Progress and Achievements	35
4.1.2 Proposed High-B R&D Activities	37
4.1.3 High-B R&D Deliverables	39
4.2 LAPPD™ MCP-PMTs	39
4.2.1 FY17 Progress and Achievements	39
4.2.2 Proposed LAPPD R&D Activities	41
4.2.3 LAPPD R&D Deliverables	41
4.3 Readout Sensors and Electronics for Detector Prototypes	42
4.3.2 Proposed R&D Deliverables	44
<b>5. Budget</b>	<b>45</b>
<b>Appendices</b>	<b>47</b>
Appendix A	
List of R&D Publications and Presentations	47

## Abstract

The EIC PID consortium (eRD14) has been formed to develop an integrated program for particle identification (PID) for a future Electron-Ion Collider (EIC) detector, for which excellent particle identification is an essential requirement. For instance, identification of the hadrons in the final state is needed for understanding how different quark flavors contribute to the properties of hadrons, and reliable identification of the scattered electron is important for covering kinematics where pion backgrounds are large. The PID systems also have the greatest overall impact on the layout of the central detector, and put important constraints on the magnetic field. It is thus essential to conduct the relevant R&D at an early stage of the development of a complete EIC detector. In addition to providing solutions addressing the broader EIC requirements, the PID consortium has worked closely with BNL and JLab to ensure that the specific R&D projects are compatible with the detector concepts that are being pursued there.

## 1. Introduction

The ability to identify hadrons in the final state is a key requirement for the physics program of the EIC. Being able to tag the flavor of the struck quark in semi-inclusive DIS can, for instance, tell us something about the transverse momentum distributions (and potentially orbital angular momentum) of the strange sea, while open charm (with subsequent decays into kaons) is important for probing the distribution of gluons in protons and nuclei. While the distribution of produced particles depends on the specific process, broadly speaking the kinematics for meson production follows the energies of the colliding beams. If the scattering produces a meson traveling in the direction of the proton (ion) beam, this meson can have a momentum which is a significant fraction (high  $x$ ) of that of the original proton (ion) beam. If the meson is produced in the opposite (electron) direction, it cannot acquire more momentum than that carried by the electron beam. In the central region, it is possible to produce a range of momenta, but the distribution is more driven by the kinematics of the process ( $Q^2, p_T$ ) than the energies of the colliding beams<sup>1</sup>. A greater reach of the PID coverage thus directly translates into, for instance, a lever arm in  $Q^2$  – a key goal for the EIC – as well as an ability to probe deeper into the high- $p_T$  region of semi-inclusive DIS. In both cases (high  $Q^2$  and high  $p_T$ ) the event rates are low, but the physics impact is high. The  $Q^2$  coverage at central angles (mid rapidity) does, however, grow quickly with momentum. To fully satisfy the physics goals of the EIC, it is thus essential to provide coverage above 5 GeV/ $c$  for hadrons ( $\pi/K$ ), with 6 – 7 GeV/ $c$  being ideal. In the electron endcap, one would need to provide hadron ID up to a significant fraction of the electron beam energy ( $\sim 10$  GeV/ $c$ ), while in the hadron endcap one would need to reach a significant fraction of the proton or ion beam momentum ( $\sim 50$  GeV/ $c$ ).

To address the different requirement associated with the three different parts of the detector, the consortium is pursuing R&D on (and requesting funding for) three different technologies for imaging Cherenkov detectors: a dual-radiator (gas/aerogel) RICH (dRICH) for the hadron endcap, a high-performance DIRC for the central (barrel) region, and a modular aerogel RICH (mRICH) for the electron endcap (which could also be used in the hadron endcap in conjunction with a single-radiator gas

---

<sup>1</sup> Note that  $p_T$  is defined with respect to the virtual photon direction in the rest frame of the proton (ion) rather than the beam direction in the detector frame. A large  $p_T$  will, generally, give rise to a higher momentum, as well as a larger component transverse to the beam, but the boost smears the distribution.

RICH such as the one developed by eRD6). A time-of-flight (TOF) measurement (or  $dE/dx$  information from a TPC) is also needed for PID in the momentum range below the thresholds of the Cherenkov detectors, for which the consortium has performed R&D on mRPC and MCP-PMT-based TOF systems.

The Cherenkov systems also have a significant potential for  $e/\pi$  identification. When combined with an EM calorimeter, the mRICH and DIRC could provide excellent suppression of the low-momentum charged-pion backgrounds which affect the ability to measure the scattered electron in kinematics where it loses most of its energy (in the detector frame). The progress of the R&D for these systems is very promising, and may in the future eliminate the needs for other supplementary  $e/\pi$  identification systems (for instance, the hadronic calorimeter on the electron endcap proposed for the BeAST or the  $e/\pi$  Cherenkov/HBD proposed for the JLab detector). Being able to eliminate such potentially redundant systems would make the EIC detector simpler, more compact, and cheaper. Further improving the  $e/\pi$  capabilities of the Cherenkov detectors may thus be a natural next step in the R&D process, and a natural extension of the current effort (for the mRICH it could mean slightly increasing the focal length and reducing pixel size, while for the DIRC it could imply improving the time resolution and ensuring that the radiator bar length could be kept as short as possible). On the hadron side, the dRICH provides a significant  $e/\pi$  identification capability ( $\sim 15$  GeV on its own and above 20 GeV with the EM cal), which is sufficient for detection of, for instance, decays of charmonium states. Here the critical question is how much of this performance, as well as the hadron ID capability, would be retained if the dimensions of the dRICH were reduced to match those of the eRD6 single-radiator gas RICH, which is currently the baseline solution for ePHENIX. A joint effort on event reconstruction and a comparison on more equal footing of the two concepts is thus a high priority.

The PID consortium is also carrying out R&D on photosensors for the Cherenkov detectors. The challenges addressed by the PID consortium are: operations inside the magnetic field of the central detector; and cost reduction. The former is carried out using the high-B test facility at JLab, while the latter focuses on adaptation and optimization of LAPPD<sup>TM</sup> MCP-PMT's to EIC requirements (pixelized readout, UV photocathodes, high-B capabilities), as well as characterization of early-production sensors. For FY18 we are also proposing to start a new effort within the consortium to develop readout electronics for all the small-pixel photosensors that will be used by the Cherenkov detectors (as well as the LAPPDs). This work will be led by U. Hawaii (which is joining the consortium) and INFN, with support from JLab. These electronics will already be used in the proposed mRICH FY18 beam test (also important for the dRICH photosensor solution), and from FY19 also for the DIRC. In the longer term, later versions of the cutting-edge electronics developed within this effort can form the basis for the readout of all Cherenkov systems of the future EIC detector.

## 2. Hadron identification

### 2.1 PID requirements and implementation options

#### 2.1.1 Hadron ID requirements

The physics program of the EIC, as described in the White Paper, the 2010 INT report, the 2015 NSAC Long Range Plan, and elsewhere, is very broad and multifaceted – and so are the corresponding detector requirements. The most basic particle distribution is that from inclusive Deep Inelastic Scattering (DIS), which essentially sums over all combinations of final-state hadrons for a given kinematics ( $x$ ,  $Q^2$ ) of the scattered electron. As one looks at specific subsets of the data, the particle distributions can be quite different. For example, the analysis of events at the exclusive limit leads to transverse spatial imaging of the quarks and gluons in the target nucleon or ion beam, for which flavor sensitivity is crucial to unravel the chiral-symmetry-breaking structure of the sea. Here, the struck quark hadronizes into a pion or a kaon, taking essentially all of the momentum transferred from the scattered electron. In this subprocess, the kaon momenta are much higher than the average momenta for kaon production in DIS. Similarly, the intermediate case of semi-inclusive DIS allows the creation of transverse images in momentum space. Here it is also important to cover a wide range in meson momentum fraction (*vis a vis* the ‘jet’), with PID for flavor separation. Failing to do so will restrict the kinematical reach of the EIC regardless of the beam energies provided by the accelerator.

Another important case to consider is when the kaons are not produced in the primary process, but are decay products of heavier mesons. For instance, the kaons from the decay of the  $\phi$ -meson, which is important for studies of gluon saturation, have higher momenta than kaons from the decay of D-mesons (open charm), which also provide information on gluon distributions.

A compilation of a catalogue of processes and kinematics illustrating the impact of various kaon identification options on the full EIC physics program goes beyond the scope of this R&D proposal. A lot of information can be found in the EIC White Paper, to which we refer. However, we note that for the purpose of understanding the general hadron ID requirements at EIC, this level of detail is not necessary. As long as one keeps in mind that a lot of the information lies in the tails of the distributions, where the number of particles is small, the meson distributions from inclusive DIS provide a good guidance. Figure 1.1.1 shows these distributions for pions and kaons in a common BNL/JLab kinematics (10 GeV electrons on 100 GeV protons), in a broad but typical bin of  $Q^2$ .

As discussed in the introduction, with higher beam energies, the meson energies in the endcaps become correspondingly higher, while the distribution in the central barrel, is less affected. Figure 1.1.1 clearly shows the need for PID over a very wide momentum range (up to about 50 GeV/ $c$ ) in the hadron endcap, and a moderate range up to 5–7 GeV/ $c$  in the central barrel. In the electron endcap, which also sees hadrons with higher momenta produced at lower values of  $Q^2$ , the desired range would reach somewhat higher than the one suggested by the  $Q^2$ -bin in Figure 1.1.1, approaching the electron beam energy. Thus, an upper limit of about 10 GeV/ $c$  is a relatively site-independent requirement. In addition, we note that the  $\pi/K$  ratios are not excessive – and tend to become smaller for higher momenta, which makes identification easier. Thus, when discussing the momentum reach, the relevant level of separation is 3–4  $\sigma$ .

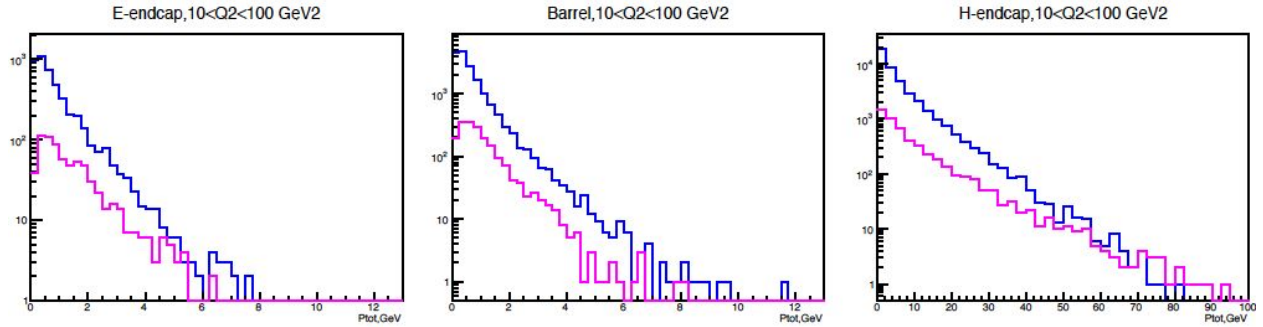


**Figure 1.1.1:** Momentum distributions of pions (blue) and kaons (magenta) from Pythia for DIS events corresponding to collisions between 10 GeV/c electrons and 100 GeV/c protons, a common BNL/JLab kinematics, shown for a bin of  $10 < Q^2 < 100 \text{ GeV}^2$  (without imposing cuts related to any specific physics channel or analysis).

### 2.1.2 Integrated PID solution for the EIC (concept) detector(s)

The three model detectors developed at BNL and JLab have slightly different layouts of the hadron ID systems, some of which have been worked out in detail, and some of which are still placeholders. The approach chosen by the PID consortium is to develop an integrated solution that would be suited for the EIC physics requirements, while maintaining a compatibility with both the accelerator energies proposed at BNL and JLab, and with the concept detectors developed there (shown in Figures 2.1.1–2.1.3).

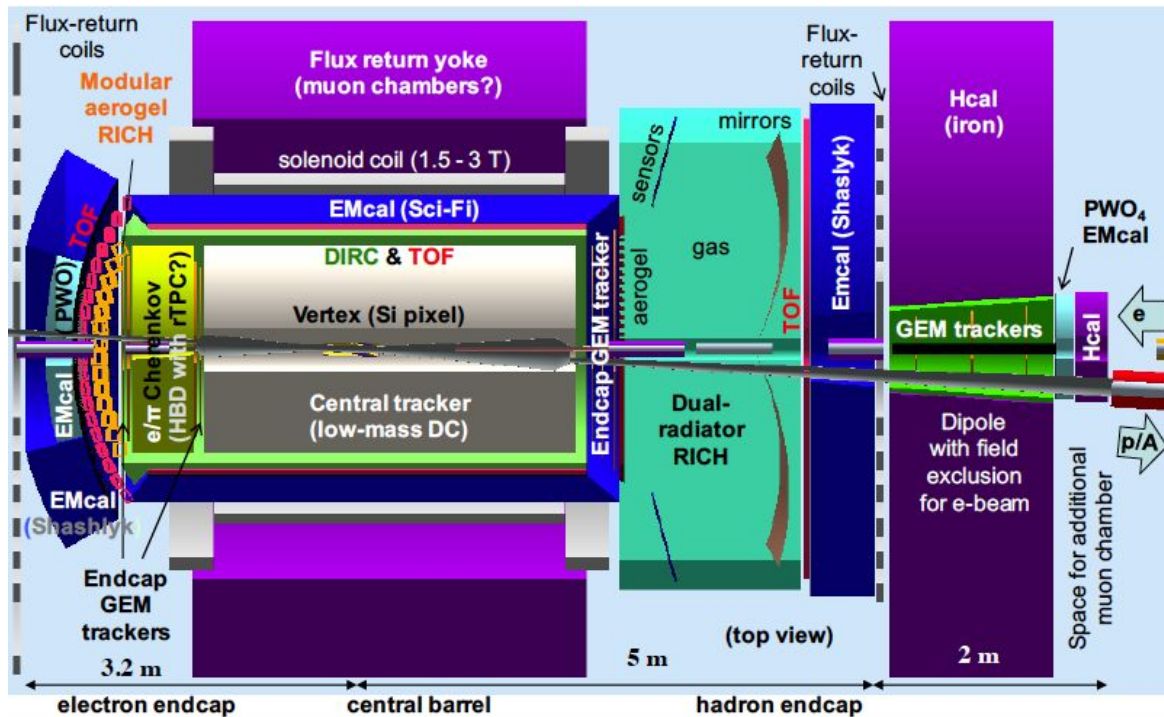


**Figure 2.1.1:** The JLab central detector concept uses the DIRC, dual-radiator and modular aerogel RICH detectors from the eRD14 R&D, and has  $4\pi$  TOF coverage. It also includes an  $e/\pi$  Cherenkov in the electron endcap for suppression of low-momentum charged pions, although the supplementary  $e/\pi$  capability of the latest version of the mRICH may turn out to be sufficient for this task.

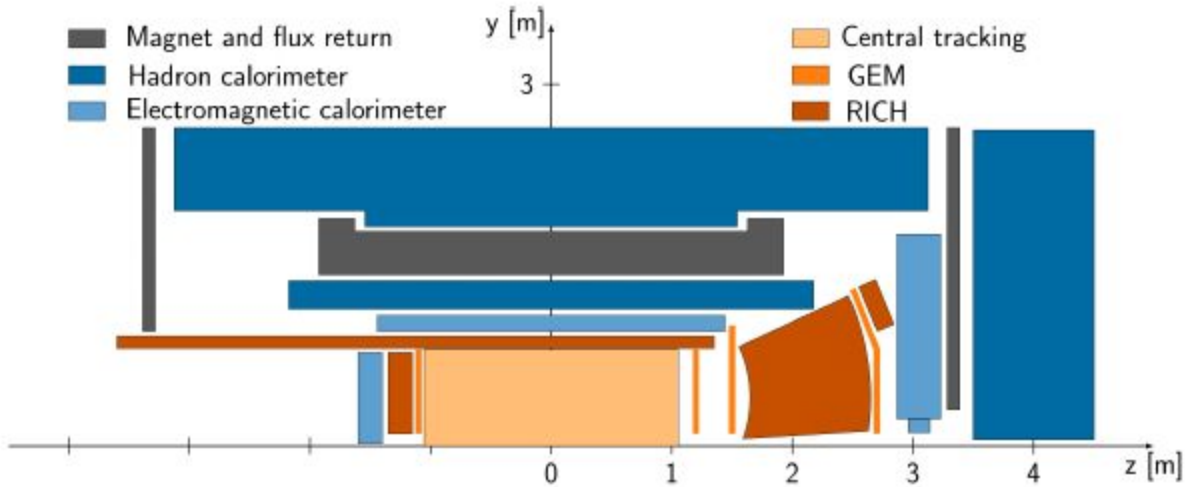


**Figure 2.1.2:** The 2017 letter of intent for forward instrumentation of the BNL sPHENIX detector, which is based on the BaBar solenoid, proposes a path for evolution towards a future EIC detector (ePHENIX) that will include a DIRC at mid-rapidity and the mRICH in the electron endcap. In the hadron endcap, the current concept uses the single-radiator gas RICH developed by eRD6 in combination with the mRICH, but is also compatible with a dual-radiator RICH, such as the one developed by eRD14.

-3.5 <  $\eta$  < 3.5: Tracking & e/m Calorimetry (hermetic coverage)

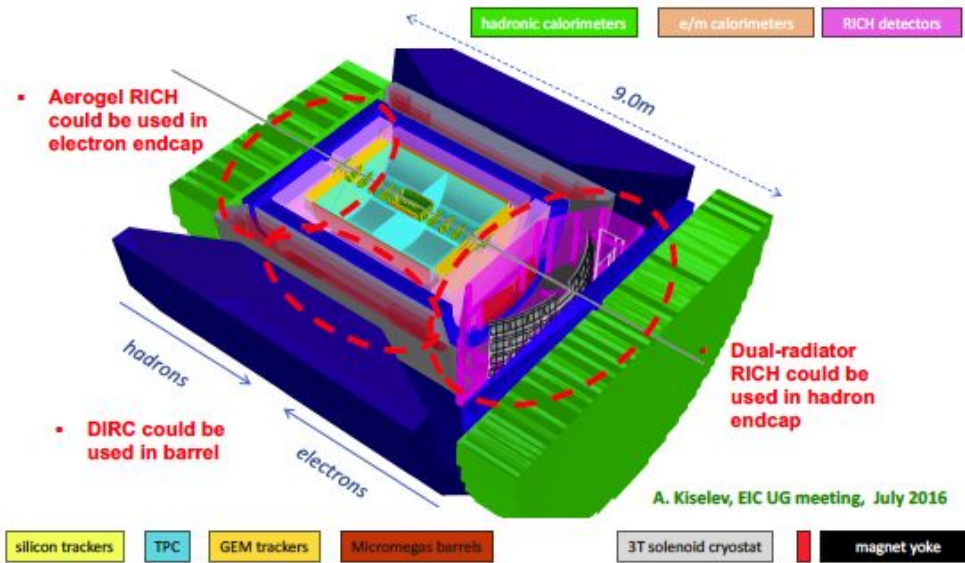


**Figure 2.1.3:** The BNL BeAST central detector concept reserves space for several types of PID systems. In its nominal configuration, it uses a RICH detector based on the one from the CBM experiment at GSI (it came with the simulation package, which is also from GSI). It would, however, be relatively straightforward to replace the CBM RICH with the dual-radiator RICH developed for the EIC by eRD14. Furthermore, the electron endcap can house the modular aerogel RICH, and the barrel can include a DIRC.

In addition to the physics requirements and the desire to reach a reasonable level of compatibility with the three model detectors, two additional criteria were also considered in the choice of subsystems: cost and space requirements.

#### Central Barrel

The decision to pursue the DIRC as the baseline solution was based on several considerations, including performance, cost, and radial space. Using recent estimates for the cost per unit area covered, polished fused silica is considerably cheaper than even the most optimistic estimates for low-cost photosensors (such as LAPPDs), making DIRC more suitable for the barrel than, say, the mRICH. The DIRC is also by far the most radially compact solution. It has already been incorporated into the design of two of the model detectors (JLab and ePHENIX), and would be straightforward to incorporate into the third one (BeAST). The ongoing R&D has also shown that performance can be pushed well beyond the state-of-the-art, from 4 GeV/ $c$  in BaBar to 5–6 GeV/ $c$  using advanced optics (eRD4) and to 6–7 GeV/ $c$  by optimizing the system for time-based reconstruction (eRD14), making it a very good match for the PID requirements for an EIC. In combination with wide bars (plates), time-based reconstruction can also help to reduce cost. A high-performance TOF is also being considered for the PID in the barrel.

#### (Outgoing) electron-side endcap

The EIC is designed to support a wide range of electron beam energies (currently assumed to be 3–12 GeV in the first stage of the JLab design and up to 20 GeV at BNL). However, hadron ID for momenta up to about 10 GeV/ $c$  would satisfy both the BNL and JLab requirements, making a compact, high-performance aerogel RICH a natural choice. Over the last year, such a system has become part of the baseline for all three major EIC detector concepts (JLab, ePHENIX, BeAST). In terms of implementation, there are three options. A mirror-based design, a proximity-focused design using two aerogel indices, and a lens-based aerogel RICH. However, the mirror-based option is not compact, and the proximity-focused alternative is only compact if the momentum coverage is modest. The lens-focused mRICH design, on the other hand, offers both a compact design and the desired momentum range. The lens-focusing also reduces the sensor area required per unit of solid angle, which is important since photosensors are the main cost driver of the RICH detectors.

#### (Outgoing) hadron-side endcap

Due to the large span of hadron momenta, ranging from a few GeV to a large fraction of the beam energy, the PID requirements on the hadron endcap are in many ways the most demanding. The difference in the maximum proton-beam energies considered at the two sites is also significant (250 GeV for BNL and 100 GeV for JLab). However, even for lower beam energies the maximum hadron momenta are so large that it is important to provide good  $\pi/K$  separation up to several tens of GeVs. Thus, any future EIC detector will need to incorporate a mirror-based, focusing gas RICH as part of the hadron-side PID solution. From a technological point of view, the R&D path that needs to be pursued for the hadron ID is thus relatively site-independent, and a nominal  $3\sigma$   $\pi/K$  coverage up to 50 GeV/ $c$  is reasonable for both sites.

The key challenge is instead how to best cover the full momentum range. The most straightforward solution is to have a dual-radiator (gas and aerogel) RICH covering the high and mid momentum range, with supplementary coverage by TOF (or  $dE/dx$ ) for the lower momenta. However, no such RICH has yet been built for a collider experiment with the strong limitations due to space and magnetic field expected

for an EIC detector. Designing such a RICH is undertaken by eRD14, employing a novel design with sector-based, outward-reflecting mirrors. However, the eRD6 has also developed a single-radiator  $\text{CF}_4$  gas RICH with inward-reflecting mirrors and a near-beam GEM-based readout (sensitive to UV only). To cover the lower momenta, the eRD6 gas RICH could be combined with an outer ring of the modular aerogel RICH detectors (mRICH, developed by eRD14) and/or with a high-resolution TOF detector. While this arrangement leaves some gaps in the coverage (low momenta at forward angles), it is important to compare the gas RICH and dRICH designs using similar reconstruction techniques and imposing similar geometric and field restrictions. Developing a slightly smaller version of the dRICH and collaborating with eRD6 on a more detailed comparison of the two approaches is thus an important goal for FY18.

*Aerogel* ( $n = 1.02$ ) |  $e_{th}(\text{GeV}/c) = 0.0025$  |  $\pi_{th}(\text{GeV}/c) = 0.67$  |  $K_{th}(\text{GeV}/c) = 2.46$  |  $p_{th}(\text{GeV}/c) = 4.89$   
*C<sub>2</sub>F<sub>6</sub>* ( $n = 1.00082$ ) |  $e_{th}(\text{GeV}/c) = 0.0123$  |  $\pi_{th}(\text{GeV}/c) = 3.48$  |  $K_{th}(\text{GeV}/c) = 12.3$  |  $p_{th}(\text{GeV}/c) = 23.4$

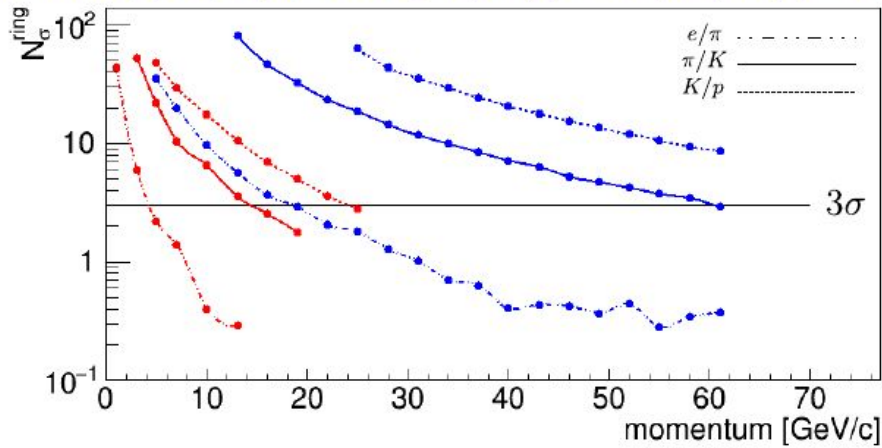


**Figure 2.1.4:**  $\text{C}_2\text{F}_6$  gas/aerogel dual-radiator RICH performance for a particle at 15 degrees. There is good overlap in PID for all three species pairs with the aerogel (red) and gas (blue).

### Time-of-Flight (TOF)

The Cherenkov detectors described above not only provide PID, but also have good timing resolution. However, they do not provide a signal for particles below threshold (*i.e.*, slower than light in the radiator medium). Thus, for PID below the range of the aerogel RICH or DIRC detectors, a different method is needed. This could be accomplished through  $dE/dx$  in the tracker or by using a dedicated TOF system. In addition to PID, the latter also offers the possibility to uniquely associate particles with a certain beam bunch (particularly important for high-frequency colliders) and to correlate particles in the central detector with near-beam hadron and electron detectors located at some distance. While a baseline capability could be provided by scintillator-based TOF detectors, mRPC and MCP-PMT based TOF systems can be highly-segmented and have the potential to provide extraordinarily good timing resolution, to levels that are competitive with AGEL and certain other Cherenkov detectors. They are also made of inexpensive materials, and R&D into construction methods could significantly lower the cost.

## 2.2 Dual-radiator RICH (dRICH)

Contacts: Z.W. Zhao <[zwzhao@jlab.org](mailto:zwzhao@jlab.org)>, E. Cisbani <[evaristo.cisbani@iss.infn.it](mailto:evaristo.cisbani@iss.infn.it)>

The goal of the dRICH detector is to provide continuous (better than 3 sigma) hadron identification ( $\pi/K/p$ ) up to about 50 GeV/c and electron identification ( $e/\pi$ ) up to about 15 GeV/c, in the (outgoing) ion-side endcap of the EIC detector, covering angles up to 25°.

We have achieved a baseline configuration for this detector (see Fig. 2.2.1 left): dual radiator (aerogel and gas) with outward reflecting mirrors in six sectors. Such a configuration with outward reflecting mirrors (as compared to inward reflecting mirrors) keeps the focal plane away from the beam and ensures that the UV photons radiated in the gas go directly to the photosensors without passing through the aerogel, where they would be otherwise scattered. The elimination of scattering of photons radiated in the gas in the aerogel is critical to achieve the needed angular resolution for high-momentum particles for which the ring image is small and the smearing needs to be kept at a minimum. With 3D focusing in each sector, this configuration also keeps the size of the total sensor area to a minimum.

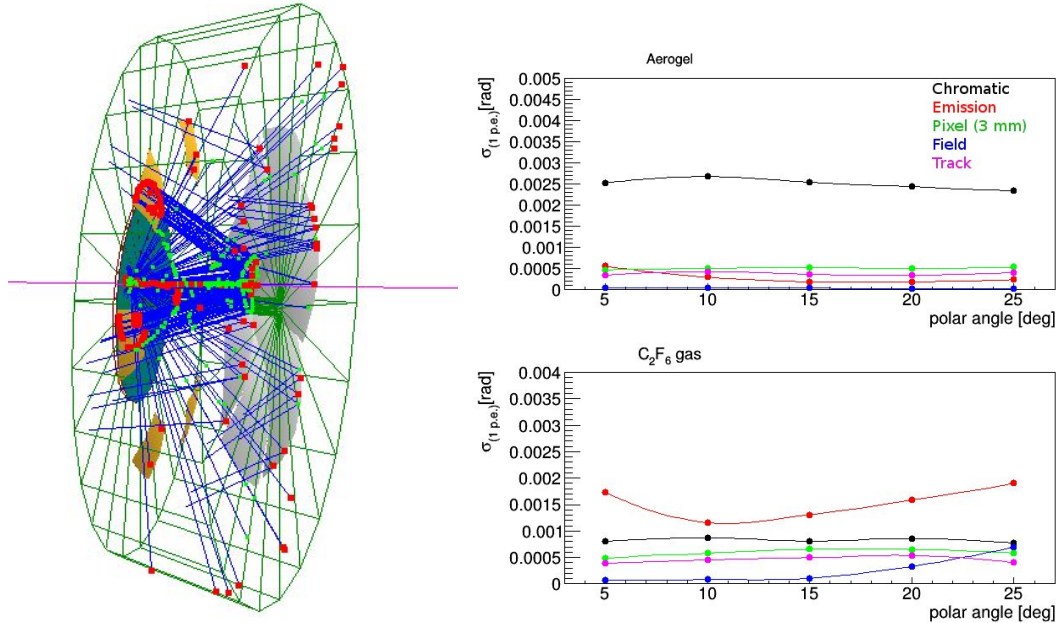


**Figure 2.2.1: Left Panel:** The GEMC based simulation of the dRICH. In transparent red is the aerogel radiator, in transparent green is the gas radiator volume; the mirror sectors are in gray and the photo-sensor surfaces (spherical shape) of about 8500 cm<sup>2</sup> per sector are in dark-yellow. A pion event of momentum 10 GeV/c is simulated. Emitted optical photons are in blue. **Right Panel:** Contributions to the single-p.e. resolution from various sources as a function of track polar angle, assuming a photo-sensor pixel size of 3 mm and an angular uncertainty of the track direction of 0.5 mrad.

The design of the dRICH fits the requirement of a generic EIC detector. It was initially developed using the geometrical constraints of the JLab EIC detector, but will in FY18 also be adapted to the slightly

smaller dimensions of the endcaps of the proposed BNL detectors and compared with the gas RICH developed by eRD6 for that geometry (in collaboration with eRD6).

### 2.2.1 dRICH Simulation and Status

The dRICH is made of six identical sectors, each with a focusing mirror and photo-detectors. Its setup is shown in the left panel of Fig. 2.2.1. We found that the best pair of radiators is aerogel ( $n(400 \text{ nm}) = 1.02$ ) and  $C_2F_6$  gas. As shown in Fig. 2.2.2, this configuration guarantees a continuous momentum coverage. The Cherenkov photons originating in the radiators of one sector can be detected by the photo-detector of another sector. The contributions of various sources to the single p.e. resolution as function of track angle are shown in the right panel of Fig. 2.2.1. The blue curves (gas) in Fig. 2.2.2 show a maximum in the momentum coverage corresponding to the minimum in the emission error for the gas radiator (see Fig. 2.2.1).

A thin acrylic slab between the aerogel and the gas guarantees at the same time filtering of the aerogel light below 300 nm (supposed to be mainly scattered photons) and insulation of the aerogel from the  $C_2F_6$  gas. The number of background photons induced by the filter is of the order of 1% of the signal for a track multiplicity of about 1. This background can be easily disentangled from the signal. The performance of the detector (using spherical shape for the photo-sensor surfaces) over the whole range of polar angles is shown in Fig. 2.2.2.

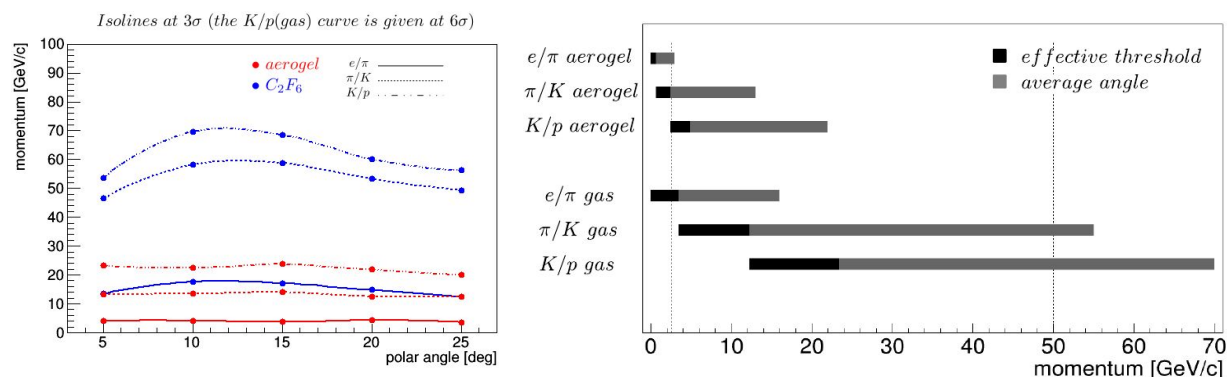


**Figure 2.2.2: Left Panel:** Isoline at three sigma: maximum momentum achieved for a PID capability greater or equal to three sigma vs. polar angle of the track. The upper  $K/p$  curve is an isoline at six sigma. **Right Panel:** Effectiveness of each radiator (PID above 3 sigma) in the central polar angles region: used in threshold mode (black bar) or in RICH mode (gray bar).

A GEMC based tessellation of the photon detector has been also introduced in the simulation. We arranged a series of  $5 \times 5 \text{ cm}^2$  tiles in a spherical-ladder-like shape as shown in Fig. 2.2.3. The tessellation of the photon detector in a non - planar shape using several planar tiles will allow the following:

1. optimization of the gas emission error (namely extend the performance of the gas radiator in the range  $[5,10]$  deg);
2. concrete arrangement for the real detector;
3. potential improvement of quantum efficiency by tilting each tile by the proper angle.

We underline that no other similar detector used such a non-planar detector surface in the past. It will

require dedicated study for alignment and arrangement of the surface.

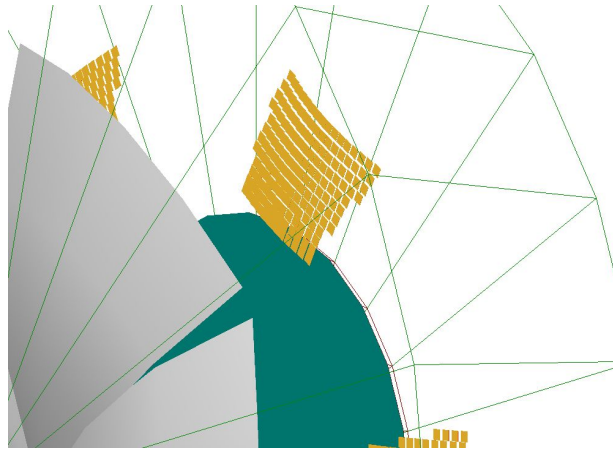


**Figure 2.2.3:** GEMC based tessellation of the detector planes.

As a first choice for photo-sensors we suggest SiPMs. They are compact, insensitive to magnetic fields, cost-effective, and can be easily arranged in different shapes. With outward-reflecting mirrors, the sensors are located in a part of the detector where the radiation levels are low, and cooling as well as strict timing cuts can be applied to reduce noise. Promising results have been obtained in the near past for SiPM in a single-photon regime<sup>2</sup>, but additional studies are needed concerning dark count and radiation hardness. Some important aspects of using SiPMs will be tested during the prototyping phases of both mRICH and dRICH. During the prototyping phase, multi-anode PMTs (H13700-03) will also be used. They have limited field tolerance, but can provide a good baseline for comparison with SiPMs during the tests.

## 2.2.2 dRICH Prototype

A quite detailed simulation study of a dRICH prototype in a minimal configuration has already started. The layout and main sources of uncertainty contributing to the 1 p.e. resolution are shown Fig. 2.2.4. For the prototype, we will exploit all the synergies with the mRICH second prototype activities. In particular, the simulated dRICH prototype uses the same photosensors (MaPMTs and SiPMs) and readout (discussed in section 4.3) as the mRICH, which can be thus shared between the two prototypes. This synergy also extends to the planned FY18 mRICH test beam, which will also be a first step in the dRICH prototyping effort.

We ask for a minimal budget for the dRICH prototype, for a mechanical tank and gas related issues. The INFN manpower assigned to the mRICH activity will also be leading the dRICH prototype realization. Aerogel, photon detectors, and electronics will be the same as for the mRICH. Depending on possible synergies with outside activities (such as CLAS12) and the capability to obtain necessary materials (*i.e.* a piece of mirror), the FY18 dRICH prototyping activities can range from testing of key concepts as part of

---

<sup>2</sup> M. Contalbrigo *et al.*, Nucl. Instrum. Meth. A **787**, 224 (2015).

I. Balossino *et al.*, Nucl. Instrum. Meth (2017), 10.1016/j.nima.2017.01.074.

the mRICH activity, to a full realization of the dRICH prototype, which could then be tested in parallel with the mRICH.

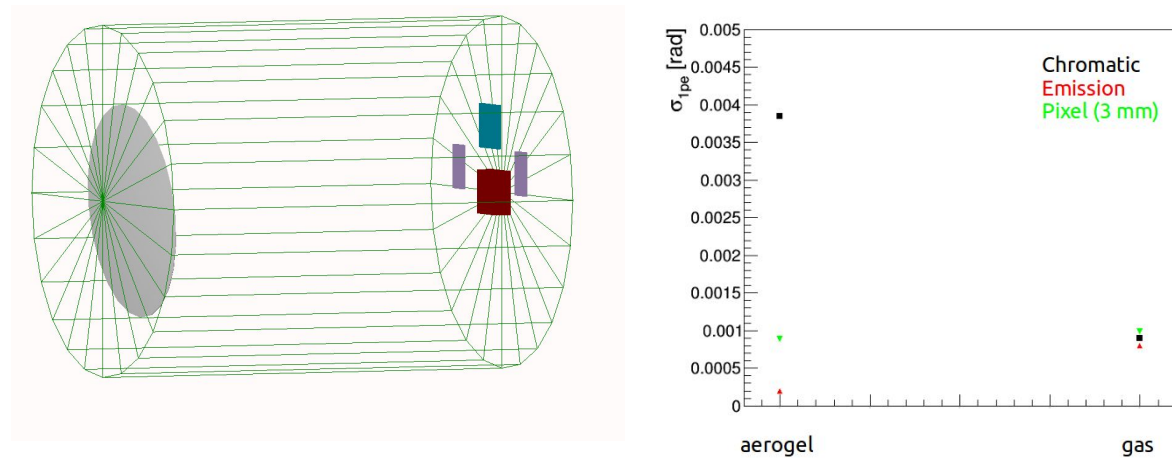


**Figure 2.2.4:** **Left Panel:** GEMC based simulation of a small scale prototype. The gas tank (green) is 1-m long and has a radius of 0.5 m. In red is the aerogel block. We use four PMTs (SiPM) to detect the whole gas ring and the same four (in a different arrangement) to detect part of the aerogel ring. A small mirror with a focal length of about 2 m is essential to disentangle the 1 p.e. error contributions for both the radiators. **Right Panel:** Main contributions to the 1 p.e. resolution for the prototype: the values have been evaluated for a particle track well above threshold (a pion at 30 GeV/c) using the Inverse Ray Tracing algorithm<sup>3</sup> and the quantum efficiency curve of the H13700-03.

### 2.2.3 FY17 Progresses and Achievements

- A baseline configuration for the dRICH has been almost completed and implemented in GEMC; an acrylic slab has been added as well as a suitable tessellation of the photon-detector surfaces.
- A preliminary minimal version of a dRICH prototype has been implemented in GEMC.
- The Inverse Ray Tracing algorithm has been used to characterize the systems.
- We have identified two options for photon detectors to be used end tested in the prototyping phases. One of them (SiPM) representing a suitable choice for the final dRICH .
- A synergy to test the dRICH principle in the ePHENIX and BeAST EIC configurations has started and will continue to be pursued in FY18.
- A publication including dRICH and mRICH has been submitted and is in press in NIM A<sup>4</sup>

### 2.2.4 Proposed dRICH R&D Activities

#### FY18:

- Study of a physics channel of interest to the EIC in the presence of physics backgrounds.
- Evaluation of the dual-radiator RICH performance in such an extended (physics) context.
- Adapt the dRICH for the geometry currently used in the BNL concept detectors (as well their

<sup>3</sup> Akopov, Norair, *et al.*, Nucl. Instrum. Meth. A 479.2, 511 (2002).

<sup>4</sup> A. Del Dotto, C.-P. Wong *et al.*, (EIC PID consortium), “*Design and R&D of RICH detectors for EIC experiments*”, NIM A (2017), In Press. <https://doi.org/10.1016/j.nima.2017.03.032>

magnetic field maps) to allow a direct comparison with the eRD6 gas RICH.

- Work on the dRICH prototype: as explained in section 2.2.2 .

#### **FY19:**

- Continuation of the activity on the dRICH prototype, if the prototype will be funded and constructed in FY18. Test beam; improved simulation based on prototype and test beam results, publication.
- Investigation of critical aspects not considered (or funded) for the first prototype: i) operation in magnetic field of the gas radiator; ii) non planar focal surface related issues; iii) precise alignment of components. iv) Further studies on aerogel: ageing and chemical interaction with gas.

#### **2.2.5 dRICH R&D Deliverables**

#### **FY18:**

- Study of the dRICH performances in an extended physics context relevant for the EIC .
- Direct comparison of the dRICH performance (after resizing) with the performance of the eRD6 gas RICH .

### **2.3 Modular Aerogel RICH (mRICH)**

*Contacts: X. He <[xhe@gsu.edu](mailto:xhe@gsu.edu)>, M. Contalbrigo <[mcontalb@fe.infn.it](mailto:mcontalb@fe.infn.it)>*

The state-of-the-art designs of imaging Cherenkov detectors, such as proximity focusing detectors<sup>5</sup>, or mirror-based imaging detectors<sup>6</sup> require substantial volumes to be able to identify particles close to 10 GeV/c momentum, due to the requirements imposed by the optical elements in the case of mirror-based detectors, or the desired ring separation in the case of proximity focusing devices. In the endcap regions of the proposed EIC detector, such space is not available. A more compact and modular design is required to fit into the available space and to still provide hadron PID capability with momentum coverage from 3 GeV/c to 10 GeV/c.

The mRICH consists of four components. A block of aerogel serves as the Cherenkov radiator. Immediately following is an acrylic Fresnel lens, which focuses the ring image and acts as a UV filter<sup>7</sup>. A pixelated optical sensor is located in the image plane, and the gap between the lens and the image plane is bounded by four flat mirrors. The device is shown in Fig. 2.3.1 (left). Also shown in Fig. 2.3.1 (right) is an event display of a 9 GeV/c pion traveling toward the center of the mRICH detector using the Geant4-based GEMC simulation framework.

---

<sup>5</sup> E. Torassa, Nucl. Instr.. Meth. **A824**, 152 (2016).

M. Tabata et al., Nucl. Instr.. Meth. **A766**, 212 (2014).

<sup>6</sup> M. Adinolfi et al., Eur. Phys. J. **C73**, 2431 (2013).

A. Augusto Alves Jr et al., J. Instrum. **3**, s08005 (2008).

J. Engelfried et al., Nucl. Instr.. Meth. **A502**, 285 (2003).

J. Engelfried et al., Nucl. Instr.. Meth. **A431**, 53 (1999).

M. Contalbrigo et al., Nucl. Instr.. Meth. **A639**, 302 (2011).

R. A. Montgomery, Nucl. Instr.. Meth. **A732**, 366 (2013).

<sup>7</sup> D.E. Fields et al., Nucl. Instr.. Meth. **A349**, 431 (1994).

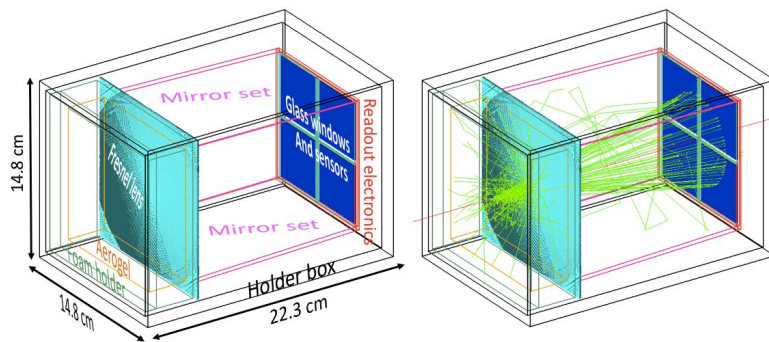


**Figure 2.3.1: Left:** The mRICH detector layout and its components. **Right:** An event display of a single 9 GeV/ $c$  pion traveling toward the center of the mRICH detector.

### 2.3.1 FY17 Progress and Achievements

In FY17, the main activities include: (1) completion of the first beam-test data analysis (see the R&D report in January 2016<sup>8</sup>). The results have been submitted to Nuclear Instruments and Methods in Physics Research Section A (currently in the final stage of the review process); (2) construction of a second prototype of the mRICH detector; and (3) implementation of the mRICH detector in the Forward sPHENIX experiment at RHIC.

#### Second Prototype

The next mRICH prototype is currently under construction at Georgia State University (GSU) (see Fig. 2.3.2). The key changes in this prototype include: (1) separation of the optical components from the readout electronics for easy integration and to avoid overheating the electronics; (2) a longer focal-length (6") Fresnel lens; (3) use of four multi-anode PMT arrays (H13700-03, 3mm  $\times$  3mm pixel size) from Hamamatsu<sup>9</sup>; and (4) use of aluminum panels for the detector frame instead of acrylic sheets to shield the external ambient light.

The new multi-anode PMT, as shown in Fig. 2.3.3, has 256 (16 x 16) channels within a 2"  $\times$  2" area and the development of the readout electronics will be the major challenge for a successful test of the second prototype. We are relying on the readout development work by the INFN (Ferrara) and University of Hawaii groups. Two H13700-03 modules were received at GSU in mid May of 2017 and two more are expected to be delivered in mid June of 2017.

<sup>8</sup> [https://wiki.bnl.gov/conferences/images/d/dd/ERD14\\_Jan\\_2017.pdf](https://wiki.bnl.gov/conferences/images/d/dd/ERD14_Jan_2017.pdf)

<sup>9</sup> Hamamatsu, 2017 Photonic Devices.

[https://www.hamamatsu.com/resources/pdf/etd/p-dev\\_2017\\_TOTH0025E.pdf](https://www.hamamatsu.com/resources/pdf/etd/p-dev_2017_TOTH0025E.pdf)

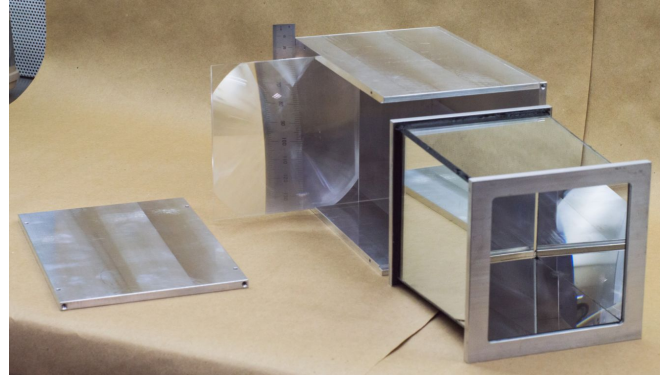
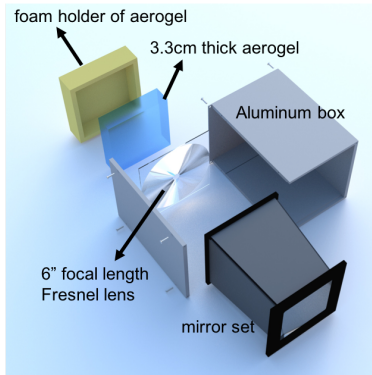


**Figure 2.3.2:** Left: 3D rendering of the second mRICH prototype. Right: The second mRICH prototype under construction.



**Figure 2.3.3:** Multi-anode PMT array (H13700-03) from Hamamatsu.

### mRICH in the Forward sPHENIX Experiment

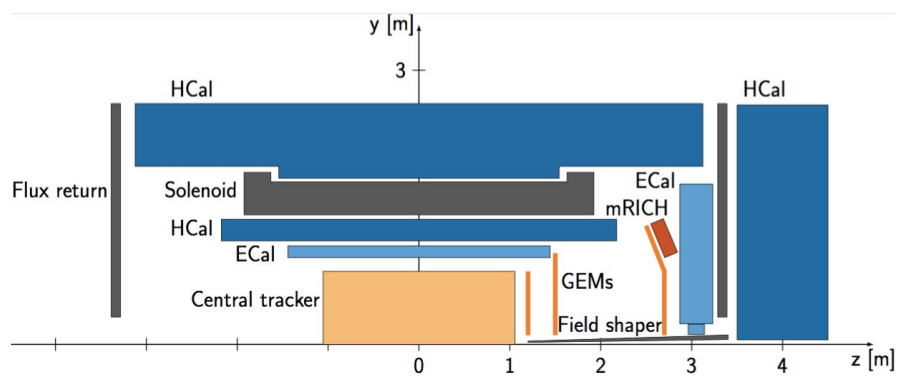


**Figure 2.3.4:** Conceptual design of the Forward sPHENIX with the mRICH detector subsystem (red). The proposed mRICH coverage spans ( $1.0 < y < 2.0$ ) in the forward region of sPHENIX.

In order to validate the mRICH detector PID performance in real experiments before EIC coming online, an implementation of the mRICH detector concept in the Forward sPHENIX has been proposed in a

Letter of Intent to BNL (as shown in Fig. 2.3.4). The addition of the mRICH detector in the Forward sPHENIX will not only enhance the physics capabilities of the sPHENIX experiment but will also make the sPHENIX detector a realistic eRHIC detector for the future EIC experiments. The mRICH detector in the forward region is the first step of upgrading sPHENIX with PID capability.

An initial implementation of the mRICH detector modules in the Forward sPHENIX detector system is shown in Fig. 2.3.5(a). There are 284 mRICH modules needed to cover the rapidity range from 1.0 to 2.0. An expanded view of the Cherenkov rings generated from two pion tracks is shown in Fig. 2.3.5(b).

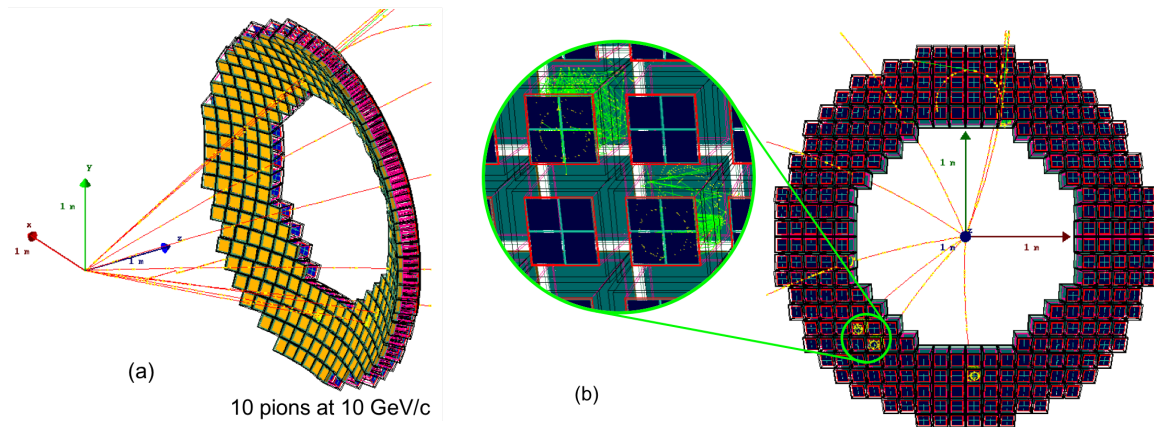


**Figure 2.3.5:** (a) The first implementation of the mRICH modules with event tracks from Geant4 simulation. (b) Expanded view of the Cherenkov ring image display from two pion tracks at 10 GeV/c.

### 2.3.2 Proposed mRICH R&D Activities

In FY 18, the proposed activities aim to deliver a second beam test, which is planned in spring 2018. With the optimized second-prototype design, the detector performance of mRICH, including  $K/\pi$  separation power and  $e/\pi$  separation below 2 GeV/c (as stated in Section 3, mRICH could be a solution for low-momentum  $e/\pi$  identification), will be studied in the second beam test.

#### FY18:

- Second beam test at Fermilab in spring 2018.
- Simulation study of mRICH performance in the Forward sPHENIX experiment at BNL.
- Simulation study of mRICH performance in the electron endcap in JLEIC.

#### FY19:

- Second beam test data analysis and publication.
- Study of a mRICH configuration using SiPM arrays with realistic cooling

### 2.3.3 mRICH R&D Deliverables

#### FY18:

- Completion of the second mRICH prototypes with a Fresnel lens and an asymmetric spherical lens, respectively.
- Performing second beam test in spring 2018.
- Detailing the performance study of the mRICH detector by simulation in the Forward sPHENIX experiment and in the electron endcap of JLEIC.

## 2.4 DIRC

Contacts: G. Kalicy <[gkalicy@jlab.org](mailto:gkalicy@jlab.org)>, J. Schwiening <[J.Schwiening@gsi.de](mailto:J.Schwiening@gsi.de)>

A radially-compact detector based on the DIRC (Detection of Internally Reflected Cherenkov light) principle is a very attractive solution for EIC, providing particle identification ( $e/\pi$ ,  $\pi/K$ ,  $K/p$ ) over a wide momentum range. The DIRC detector is a special kind of RICH counter using rectangular-shaped radiators made of synthetic fused silica that are utilized also as light guides to transport Cherenkov photons to an expansion volume, where they are recorded by an array of photon sensors. During the photon transport, the emission angle of Cherenkov photons with respect to the particle track is maintained and can be reconstructed from the measured 3D parameters: the image location on the detector surface ( $x$ ,  $y$ ) and the time of arrival of each photon ( $t$ ).

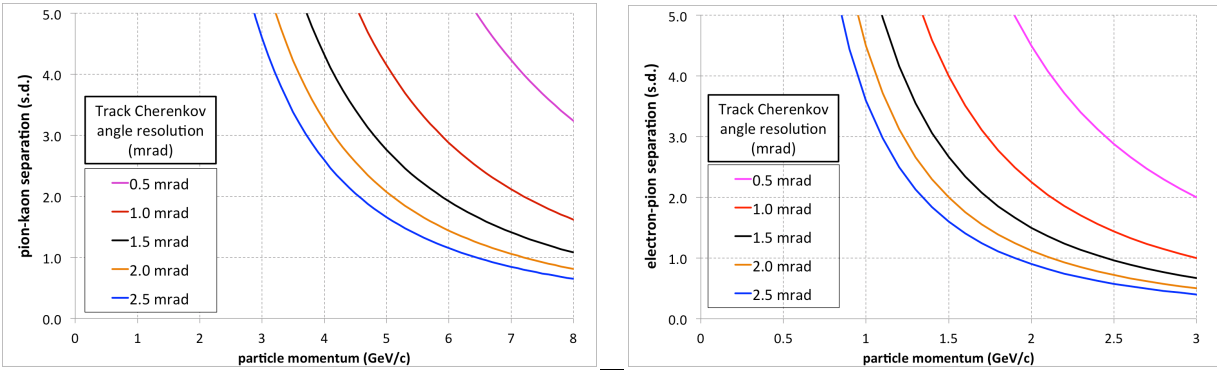


**Figure 2.4.1:**  $\pi/K$  separation (left) and  $e/\pi$  separation (right) in the DIRC in units of standard deviations (s.d.) as function of particle momentum for different values of the track Cherenkov angle resolution  $\sigma_c^{track}$ . A track Cherenkov angle resolution of 1 mrad is required to achieve 3 s.d.  $\pi/K$  separation at 6 GeV/c and 3 s.d.  $e/\pi$  separation at 1.7 GeV/c.

Figure 2.4.1 shows how the maximum momentum goal for  $\pi/K$  and  $e/\pi$  separation translates into the required Cherenkov angle resolution. In an EIC, the pion background for kaons varies with reaction channel and kinematics, but in general a 3 s.d. criterion is relevant. Achieving 3 s.d. separation using fused silica radiator bars requires a Cherenkov angle resolution of 1.3 mrad at 5 GeV/c and 1.0 mrad at 6 GeV/c. Achieving this resolution assumes that the central tracker will be able to provide an angular resolution at the sub-mrad level (*i.e.*, comparable to the CLAS12 forward detector). The R&D undertaken

by the EIC PID consortium achieved the goal<sup>10</sup> of showing the feasibility of a high-performance DIRC that would extend the momentum coverage well beyond state-of-the-art, providing 3 s.d. separation of  $\pi/K$  up to 6 GeV/c,  $e/K$  up to 6 GeV/c,  $e/\pi$  up to 1.7 GeV/c, and  $K/p$  up to 10 GeV/c.

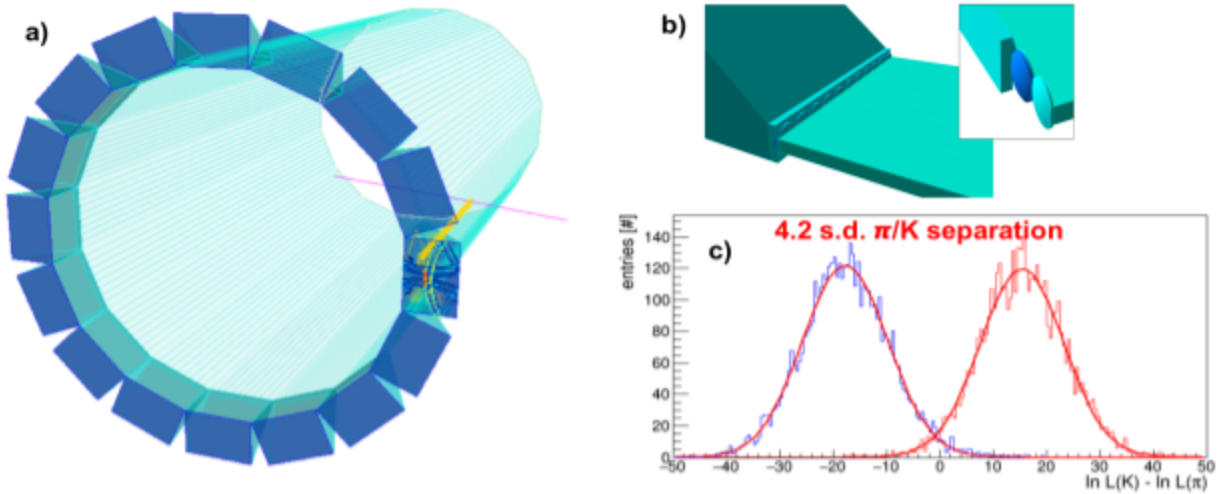


**Figure 2.4.2:** a) Geant4 geometry of the high-performance DIRC. b) The fused silica prism expansion volume, a row of spherical three-layer lenses with high index of refraction (no air gaps) and the radiator bars. The insert shows the individual lenses and layers of the spherical lens system. c) Example of the time-based imaging-based performance capability of high-performance DIRC. Log-likelihood difference for kaon and pion hypotheses for a sample of 6 GeV/c pions and kaons at 30° polar angle. The  $\pi/K$  separation power extracted from the Gaussian fits is 4.2 standard deviations.

The outcome of the simulation effort in FY16 was the initial design of the high-performance DIRC with narrow bars and spherical 3-layer lenses, shown in Fig 2.4.2a and 2.4.2b. Using the time-based imaging reconstruction, it was shown that, assuming a realistic timing precision of 100ps per photon, this design is capable of reaching 4.2 s.d.  $\pi/K$  separation at 6 GeV/c and 30° track polar angle (Fig 2.4.2c).

### 2.4.1 FY17: Progress and Achievements

The activity focus in FY17 was on the evaluation of the radiation hardness and focal properties of the spherical 3-layer lens prototype. The outcome was the confirmation of crucial parameters of the lens, in particular the flat shape of the focal plane for many photon angles. This 3-layer lens also performed very well in the PANDA Barrel DIRC prototype during tests with particle beams. First results of the radiation hardness suggest that NLaK33, used as a middle layer of this lens, is not radiation hard enough for the EIC DIRC and that an alternative material has to be used in future prototypes of the lens. The results described below have a direct impact on the priority of simulation and reconstruction effort for FY18 and the next stage of the development of the radiation hard 3-layer lens.

<sup>10</sup> G. Kalicy *et al.*, *High-performance DIRC detector for the Electron Ion Collider*, JINST 11 no.07, C07015 (2016). DOI: [10.1088/1748-0221/11/07/C07015](https://doi.org/10.1088/1748-0221/11/07/C07015)

## Hardware: Development and Validation of the 3-layer Spherical Lens

### Results of the FY17 data analysis of test beams at CERN

The analysis of the data obtained during two PANDA Barrel DIRC test beams at CERN in 2015 and 2016 was concluded in FY17. The beam test in 2015 was primarily dedicated to measurements using the narrow bar with the 3-layer spherical lens procured in FY14 and MCP-PMTs with a pixel size of about 6 mm. The analysis of the data collected during this run was completed in FY17, including a detailed error evaluation and a per-sensor calibration of the Cherenkov angle.

The test beam at CERN in October/November 2016 was primarily focused on the validation of the PID performance of the geometry using wide radiator plates, with and without a cylindrical lens. The radiator plate was coupled to the cylindrical 2-layer lens or directly to the synthetic fused-silica prism expansion volume, which had a  $30^\circ$  opening angle. The time-based imaging method was used to evaluate the PID performance. Figure 2.4.3 shows results of the time-based imaging method applied to data taken in 2015 with the narrow bar geometry and in 2016 with the wide plate geometry. The narrow bar with the 3-layer spherical lens proved to be more robust in terms of timing precision and backgrounds than the wide plate with the 2-layer cylindrical lens and provided superior  $\pi/K$  separation.

A new 3-layer cylindrical lens was designed and procured in FY17 for use in the next CERN beam test, scheduled for August/September 2017, where we plan to test the performance of designs using narrow bars or wide plates, in combination with a new fused silica prism with an opening angle of  $33^\circ$ , close to the prism angle for the high-performance EIC DIRC.

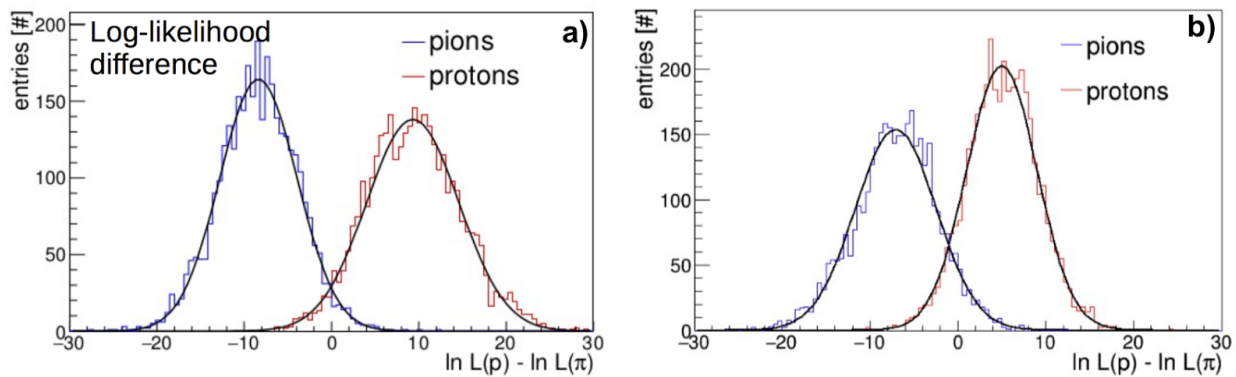


**Figure 2.4.3:** Example results of the PANDA Barrel DIRC prototype test at CERN. The time-based imaging method is used to calculate the log-likelihood difference distributions. The corresponding  $\pi/p$  separation power at a momentum of  $7 \text{ GeV}/c$  and a polar angle of  $25^\circ$  is 3.6 standard deviations (s.d.) for data taken in 2015 with the narrow bar geometry (a), and 3.2 s.d. for data taken in 2016 with the wide plate geometry.

### Mapping the focal plane of the 3-layer spherical lens

The schematic of the setup designed and built in the Old Dominion University laser lab to measure the shape of the focal plane of the 3-layer lens was placed on a rotating stage and rotated through two parallel laser beams. The intersection point of the two laser beams determined the focal length. The lens was placed inside a  $30 \times 40 \times 60 \text{ cm}^3$  glass container filled with mineral oil (with a refractive index very close

to fused silica) to simulate the focusing behavior of the lens placed between the bar and the prism. The 3-layer lens is supported in a special 3D-printed holder that makes it possible to map out the focal plane in all three dimensions, which will be particularly important for comparing spherical and cylindrical lens designs. In addition, the lens can be shifted in  $x$  and  $y$  to measure the focal distance when the laser beam is off-center of the lens. Results of that measurement were compared to the prediction from the GEANT4 simulation. Figure 2.4.4 shows three example results, confirming that the measured shape of the focal plane is in good agreement with the simulation, both for the 3D rotation and for the lasers going off-center through the lens. Additional results can be found on the eRD14 wiki<sup>11</sup> where measurements for other rotation angles and off-center laser beam positions are compiled. The spherical lens produces the desired flat shape of the focal plane if the beam goes close to the center of the lens. Due to lens aberrations, the shape starts to slightly bend when the beam is shifted off-center but the simulation still predicts the shape well and the focal plane shape is still much more flat than a traditional single-layer lens.

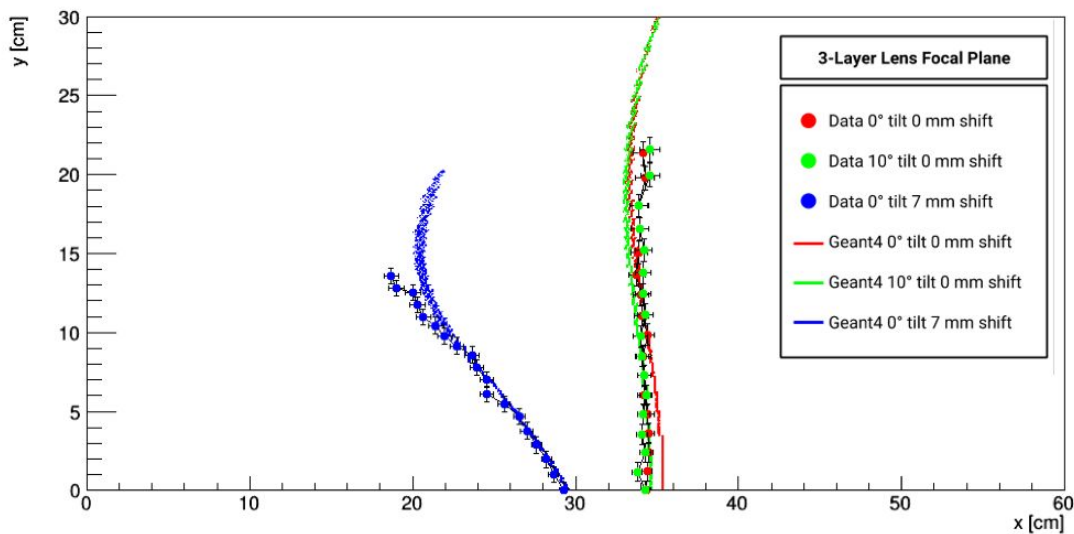


**Figure 2.4.4:** Measured shape of the focal plane (points) compared to simulation (solid lines) for two different azimuthal tilts and horizontal shift of the lens. The  $x$  coordinate corresponds to the focal length and the  $y$  coordinate to the focal point location perpendicular to the incident beams, calculated for different lens rotation polar angles.

### Radiation Hardness Measurement

The determination of the radiation hardness of materials is an important aspect of the EIC DIRC R&D. Synthetic fused silica, which is used for most of the optical components in all DIRC systems, was already extensively tested for the BaBar and PANDA DIRC counters and proved to be radiation hard. However, the middle layer of the 3-layer lens is made of a high-refractive index lanthanum crown glass, NLaK33, which had yet to be tested for radiation hardness.

The irradiation is being performed at Catholic University of America in an X-ray setup with energies up to 160 keV. The dose is accumulated in small steps, delivering a dose of 50–100 rad at a time. Between each step, the transmission properties of the lens and a pure NLaK33 sample will be measured in a monochromator setup with a reproducibility of 0.2% to quantify the impact of the radiation.

<sup>11</sup> [http://phynp6.phy-astr.gsu.edu/eRD14/index.php/Mapping\\_Focal\\_Plane](http://phynp6.phy-astr.gsu.edu/eRD14/index.php/Mapping_Focal_Plane)

To disentangle the radiation damage effects of the composite materials (synthetic fused silica, NLaK33, epoxy glue, anti-reflective coating), a pure NLaK33 sample was studied first. A synthetic fused silica sample serves as a reference in the monochromator to remove systematic errors from the NLaK33 measurement. The 28x28x8 mm<sup>3</sup> sample of NLaK33 material was irradiated in the X-Ray setup set to 160 keV and 6.2 mA. The dose is collected over 1–2 repetitions of irradiation lasting 7.5 s each, around 25 rad each. First results are shown in Fig. 2.4.5. The transmission drops significantly at a rate of around 1.3% per each 100 rad at 420 nm wavelength.

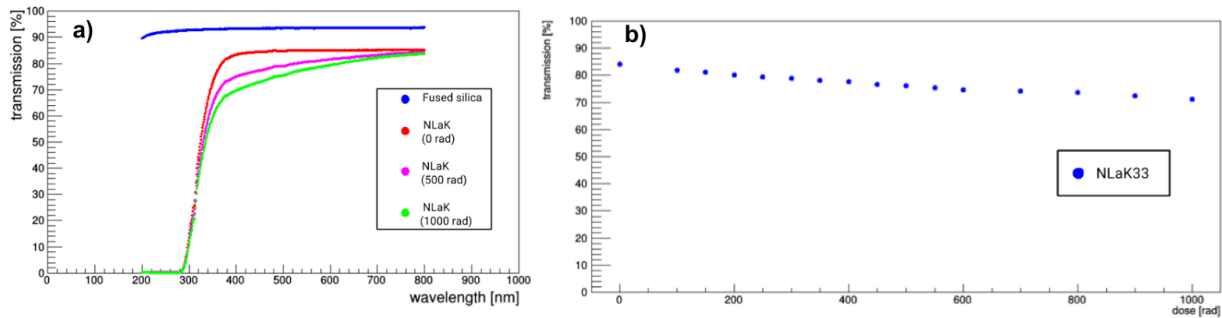


**Figure 2.4.5:** Measured transmission (not corrected for Fresnel losses) through the NLaK33 sample and the fused silica reference sample as a function of wavelength (a) and irradiation dose for 420 nm (b).

### Software: Simulation and Reconstruction

The planned activities on the detailed GEANT simulation and the time-based imaging algorithm had to receive a lower priority since the FY17 budget did not provide the requested funding for the new PostDoc. Aspects of the work, in particular the simulation of the new 3-layer cylindrical lens and minor improvements to the time-based imaging method, were shifted to GSI. However, new detailed studies, such as the optimization of the design in simulation, including a comparison of narrow bars to wide plate, the mitigation of the chromatic errors, the DIRC event timing, and the evaluation of the combined PID system, had to be postponed to FY18.

### 2.4.2 Proposed DIRC R&D Activities

Initial results of the radiation hardness of the NLaK33 material showed a significant transmission loss at rather modest doses, making it unsuitable for the EIC DIRC. This motivates the search for alternative materials for the final design of the lens for the high-performance DIRC at EIC. Furthermore, to conclude the evaluation of the NLaK material, we plan to finish the X-ray studies using thinner NLaK samples, matching the depth-of-penetration of the X-ray source, and to irradiate additional samples with Co<sup>60</sup> and neutron sources. The same sources will be used to study the radiation hardness of alternative lens material candidates. For FY18 we plan to obtain material samples from industry and to study them on test benches. In addition, we plan to measure wavelength-dependent transmission of the various materials used in DIRC detector, *e.g.* silicones, glues, radiation hard glasses. Results from these measurements will be implemented in Geant4 to study lens- and mirror-based designs that meet radiation hardness requirements for EIC.

The new cylindrical 3-layer lens prototype, procured with FY17 funds, is currently being fabricated by industry. Delivery is expected by August 2017, in time for inclusion in the upcoming PANDA Barrel

DIRC test beam at the CERN PS in Aug/Sep 2017, where the performance of the lens will be evaluated in combination with narrow bars and wide plates. The participation in this beam test, as well as the analysis of the beam data, are important activities planned for FY18.

We are in the process of negotiating the possible transfer of legacy components used for the BaBar DIRC and the FDIRC from SLAC to ODU or JLab. This includes the setup used for 2D scans of multi-anode PMTs and MCP-PMTs and elements of the Cosmic Ray Telescope. Although some of the components and software may require a substantial effort to be used for the eRD14 R&D, this will provide significant long-term benefits to future DIRC tests and more advanced studies of its components and prototypes.

The primary capital investment item for FY18 is the procurement of a PHOTONIS Planacon XP85122-S MCP-PMT. This sensor is currently the only commercially available high-B field tolerant option for the small-pixel readout of the DIRC. With a MCP pore size of 10  $\mu\text{m}$ , an array of 32 x 32 readout pads (corresponding to a pixel pitch of 1.6 mm), and a sapphire front window, it matches the benchmarks for potential high-performance DIRC sensors. The performance of this sensor would be evaluated in FY18 and FY19 with light from the picosecond laser pulser, procured by ODU, possibly using the SLAC PMT scanning setup or the Hawaii waveform-sampling readout electronics. Tests of the timing resolution, charge sharing, gain and photon detection efficiency of this sensor would provide valuable experience and prepare the DIRC project for the next stage in designing a full-size prototype.

Due to limitations in the FY17 budget, many software activities had to be postponed to FY18. One of the highest-priority software tasks for FY18 is the further development of the time-based imaging method, in particular the analytical calculation of the probability density functions, required for applying this algorithm to experimental data. After an initial design for the high-performance DIRC was simulated in FY16, it is now crucial to study the effect of different bar sizes, focusing system options, expansion volume shapes and dimensions, as well as sensor types (MCP-PMTs vs. SiPMs) and pixel sizes on the DIRC performance to identify a credible and cost-efficient baseline design for the high-performance DIRC. The implementation of this design in a full EIC central detector simulation framework is an important step to facilitate the study of the combined PID performance of the eRD14 detector systems. Since the DIRC system is compatible with all three concept detectors, this activity should start with a first detector framework example in FY18 and conclude with integration into all three frameworks in FY19. Other important simulation activities are the study of the mitigation of chromatic dispersion effects using fast timing and the potential use of the DIRC for precise event timing.

After the ODU Ph.D. student on the DIRC project graduates in 2017, a new PostDoc at CUA, supported by eRD14 funding, will take over many of his responsibilities, including the EIC DIRC simulation, test-beam data analysis, and lens measurements, and will add new capabilities to the project. A candidate for the CUA PostDoc position was selected and the hiring process has started. We expect the PostDoc to participate in the upcoming DIRC beam test at CERN in Aug/Sep 2017 and to spend time at GSI to work on the simulation. Furthermore, we hope to add at least one new Ph.D. student to the project, using university funding.

### **Synergetic Activities Supported by External Funding**

The synergy with the PANDA Barrel DIRC project not only provided access to the prototype and the CERN test beams in 2015, 2016, and 2017 but includes several planned mid- and long-term contributions from the GSI DIRC group to the EIC DIRC project. With the submission of the PANDA Barrel DIRC TDR in 2017 the activity focus of the GSI DIRC group on PANDA will shift to the mechanical design and the R&D for the detector assembly. Both activities are directly relevant to the EIC DIRC design.

After conclusion of the beam tests of the PANDA Barrel DIRC, components of the prototype are expected to become available for use by the EIC DIRC effort during FY19/FY20 on the basis of a long-term loan or an in-kind contribution. The mechanical prototype structure, as well as one narrow bar, one wide plate, and a prism expansion volume, could be transported to the U.S. for prototype beam tests at JLab or Fermilab. This would significantly reduce the financial investment required to set up the first prototype for the test of lenses, sensors, and readout electronics with particle beams (this would be a deliverable in FY20/FY21).

### **Proposed activities**

#### **FY 18**

- Software: Development of analytical version of time-based imaging.
- Software: Cost/performance study to identify optimum bar, pixel, and expansion volume size as well as different focusing system for future baseline design.
- Software: Implementation of baseline design into ePHENIX detector simulation framework.
- Software: Investigation of chromatic dispersion mitigation in the context of different photocathode materials and readout timing precisions.
- Software: Investigate potential use of DIRC for high-precision event timing.
- Software/Hardware: Evaluation of cylindrical 3-layer lens using the 2017 CERN test beam data and lasers in optics setup.
- Software/Hardware: Study of optical properties and radiation hardness of various DIRC materials in simulation and using obtained samples and X-ray, Co<sup>60</sup>, and neutron sources and the monochromator at CUA.
- Hardware: Procurement of Planacon XP85122-S sensor and evaluation of performance for DIRC.

#### **FY 19**

- Hardware: Phase 0 of dedicated DIRC@EIC prototype development (modified PANDA DIRC prototype, possible in-kind contribution from GSI).
- Software: Optimization of design in coordination with the other eRD14 PID systems within full EIC central detector simulation framework.
- Software: Study PID performance of the baseline design in the presence of backgrounds.

### **2.4.3 DIRC R&D Deliverables**

#### **FY18**

- Cost-optimized baseline design of high-performance DIRC, implementation into ePHENIX detector simulation framework.
- Define sensor and electronics requirements for high-performance DIRC using both geometrical and time-based reconstruction.

- Performance evaluation of cylindrical 3-layer lens on test benches and in particle beam.
- Study radiation hard alternative materials for the next prototype of 3-layer lens.
- Publication summarizing tests of the 3-layer lens.

#### FY19 (tentative)

- Evaluation of DIRC performance in the context of the combined PID systems in full EIC central detector simulation framework.
- Evaluation of the impact of event- and track-related backgrounds on the PID performance.

## 2.5 High-resolution Time-of-Flight (TOF)

Contacts: M. Chiu <[chiu@bnl.gov](mailto:chiu@bnl.gov)>, M. Grosse-Perdekamp <[mgp@uiuc.edu](mailto:mgp@uiuc.edu)>

High-resolution TOF provides an attractive solution for PID covering the lower momenta range at the EIC, below the turn on threshold for gas Cerenkov detectors. The R&D pursued here intends to push the state of the art of two technologies, MCP-PMT and mRPC, with an ultimate goal of 5 and 10 ps, respectively. Assuming a total resolution of 10 ps and a distance of 1 m, TOF could achieve  $3\sigma$  separation for  $\pi/K$  and  $K/p$  of 3.5 and 6 GeV, respectively, which would be adequate for mid-rapidity PID. In the hadron going direction, where the TOF wall could be placed 3 m from the interaction point, the  $3\sigma$  separation for  $\pi/K$  and  $K/p$  would be 6.5 and 11 GeV. Coupled with a  $dE/dx$  measurement from a TPC, TOF would also provide electron identification up to several GeV. Besides providing PID, TOF enables bunch association which is required since each bunch may have a different polarization.

### 2.5.1 FY17 Progress and Achievements

While high performance TOF was not funded during the past cycle, our group has continued some development as available resources have permitted. During the past year a major thrust was to study in more detail the issue of where the start time ( $t_0$ ) for a TOF detector at the EIC could come from. One solution would be to install high performance TOF everywhere ( $4\pi$ ); then the start time could be almost trivially obtained by measuring the electron's  $t_0$ . Another possible solution would be to install an inner silicon tracking layer that is capable of 10 ps time resolution. Such silicon tracking detectors are currently being developed for the HL-LHC, using technology such as LGADs (Low-Gain Avalanche Diodes)<sup>12</sup>.

However, even without an independent measurement of the  $t_0$ , it seems possible to derive the start time using the tracks measured in the TOF wall itself. A start time  $t_{\text{start}}$  for each of the  $N$  particles in the TOF acceptance is determined using  $t_{\text{det}} - t_{\text{start}} = t_{\text{flight}} = (L/c)[1+(m/p)^2]^{1/2}$ , where  $t_{\text{det}}$  is the measured time in the TOF detector and  $L$  is the path length from the vertex to the detector. A priori one does not know the particle's ID, but one can assume they are either pions, kaons, or protons. Electrons and muons are either a small background or assumed to be identified separately. With  $N$  particles, there are  $3^N$  combinations possible, and each combination gives a different set of start times. By selecting the combination that gives

<sup>12</sup> LGADs have been tested by Atlas to 10 ps resolution before irradiation, but reduce to 30 ps after being irradiated to levels expected at the HL-LHC. See J. Lange *et al.*, *Gain and time resolution of 45  $\mu\text{m}$  thin Low Gain Avalanche Detectors before and after irradiation up to a fluence of  $10^{15}$  neq/cm<sup>2</sup>*, JINST 12 no.05, P05003 (2017). <http://dx.doi.org/10.1088/1748-0221/12/05/P05003>

the smallest variance in the set of start times, we find that in a PYTHIA Toy MC one can select the right PID combination 99% of the time, and from that combination extract a best  $t_0$  with a resolution comparable to the assumed TOF resolution (10 ps), as seen in the right hand plot of Fig. 2.5.1. A toy MC leaves out a lot of realistic effects, especially background tracks from fake or misidentified tracks. The left two plots of Fig. 2.5.1 show the results of this algorithm on PHENIX data in Au+Au collisions using the PHENIX TOF.E detector, which has an intrinsic resolution of  $\sim 150$  ps. The self determined  $t_0$  in PHENIX data is compared to the independently measured  $t_0$  from the PHENIX BBC. Agreement is good, with a resolution of about 150 ps which is comparable to the detector resolution. Here, a tail of mis-measured start times is also evident at the level of  $O(10\%)$  due to mis-measured tracks. In the high multiplicity heavy-ion collision environment, the level of mis-measured tracks can easily exceed 10% and these nuisances can distort the self-extracted  $t_0$ .

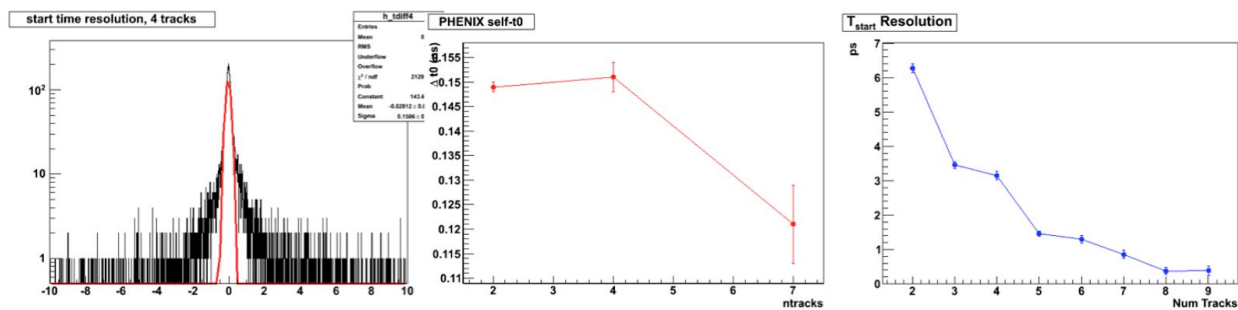


**Figure 2.5.1:** Self-derived start time distribution for 4 track events in the PHENIX TOF.E compared to BBC  $t_0$  (left), and from PHENIX TOF.E data (center) as well as from PYTHIA 6.428 e+p Toy MC (right) as a function of the number of reconstructed tracks.

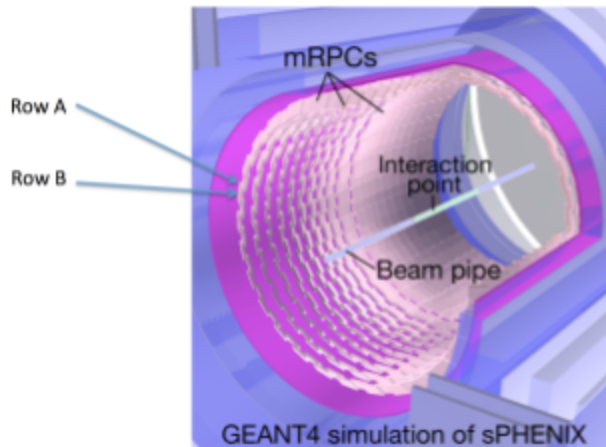
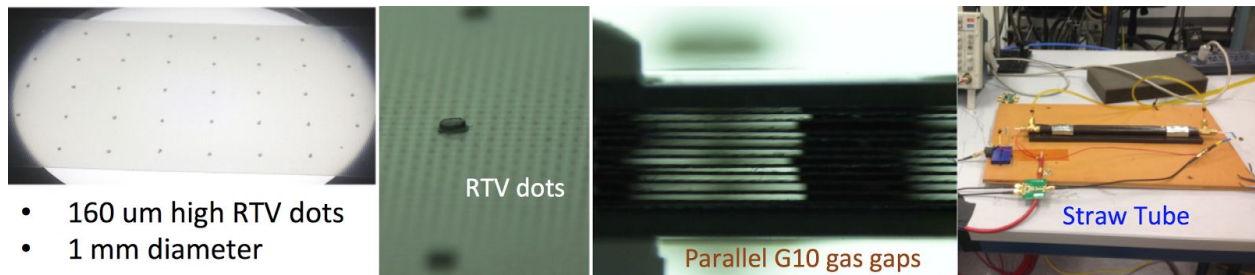


**Figure 2.5.2:** mRPCs implemented in the sPHENIX simulation as a barrel TOF system. The inner silicon tracking and TPC have been suppressed when drawing in order to show the projective mRPC modules.

The number of fake tracks is expected to be much lower in  $e^+p$  collisions, but this has to be verified. To do this, a mid-rapidity mRPC TOF wall has been fully implemented in the sPHENIX Geant4 simulation. Besides allowing studies of all the realistic effects expected at the EIC, the implementation proves that a mRPC TOF wall fits in a radial space of only 10 cm and the modules can be oriented so that they are projective towards the interaction point, as seen in Fig. 2.5.2. Unfortunately, the sPHENIX tracking

software has been under development the last couple of months so a full simulation of the self-extracted start time has not been possible. However, the tracking software is almost done, and it should be possible to complete the study soon. From preliminary discussions with the experts, the tracking in sPHENIX for e+p collisions should have fake tracks at the level of a few percent at most, and thus not suffer some of the problems seen in PHENIX from heavy ion collisions. Besides the  $t_0$  studies, the psTOF group has continued to work on building an mRPC with more gas gaps by using thinner dielectrics. Previous work demonstrated for the first time with 100  $\mu\text{m}$  mylar sheets that with the right support, even flexible dielectrics could be used in mRPCs. During the spring, an undergraduate SULI student at BNL pursued this further by “silk-screening” 160  $\mu\text{m}$  high, 1 mm diameter RTV spacers every cm on 100  $\mu\text{m}$  thick G10 sheets. This was used to produce a mRPC with reasonably uniform gas gaps (see Fig. 2.5.3). The RTV dots are expected to have a very high resistance due to their small size and high volume resistivity, so that the dielectric material remains electrically floating. G10 is a material that is much less electronegative on the triboelectric scale and therefore will not charge up statically, as was the case for mylar. Recently, however, our group has discovered the wide availability of “cheap” 100  $\mu\text{m}$  tempered glass, which is used extensively in smartphone screen protectors. We are in the process of acquiring some and expect this might prove the ideal mRPC material. They are semi-flexible, but we believe there should be no problem producing stable, uniform gas gaps with them based on our recent experience with flexible materials.



- 160  $\mu\text{m}$  high RTV dots
- 1 mm diameter

**Figure 2.5.3:** Work done with SULI undergraduate student during spring semester in psTOF Lab at BNL. The studies above provide a foundation for further studies over the summer and coming year.

The student also developed prototype straw tube trackers that are to be the basis for tracking cosmic rays in the lab. Previously our group hoped to develop standalone silicon trackers for cosmic ray tracking, but with personnel changes at BNL it was impossible to finish that development. The tracking of cosmic rays is essential to study the dependence of the time resolution on the angle of the cosmic, and perhaps more importantly, the dependence on the hit position on the strip, which may be one of the factors limiting the timing resolution of mRPCs.

## 2.5.2 Proposed TOF R&D Activities

Within eRD14 (and previously eRD10), our group has demonstrated that a resolution of  $\sim 20$  ps is achievable with glass mRPCs by using thinner glass, making smaller gas gaps (up to some minimum level around 100  $\mu\text{m}$ ), and increasing the number of gaps. Our previous results confirms earlier results from C. Williams *et. al.*, and is only the 2nd set of mRPCs to achieve such resolutions. To achieve even better resolution for the mRPC, we have proposed that one solution is to replace the glass with even thinner

dielectrics and thus increase the number of gas gaps. We believe a mRPC with 48 gas gaps is possible in the same space as the 24 or 36 gap mRPCs from C. Williams and eRD14, respectively.

Other limits to the timing resolution may come from a dependence of the timing on the hit position of the particle on the strips. The strips are 1 cm wide, which is greater than the 10 ps equivalent of 3 mm. A tracker system is being developed for use in the lab to be able to study the position dependence of the timing resolution. The major impediment to being able to do this study (and all other mRPC studies) efficiently is the lack of more scalable electronics for our testing. We currently use TI amplifier evaluation boards for preamps with the DRS4 evaluation board for digitization for a total of 4 channels. With this setup, we can only read out 1 strip on a pair of mRPCs, since we read out both ends of the strip on the two detectors.

With custom preamp boards that are designed to match the spatial constraints of the mRPC, and a custom DRS4 digitizer board, we should be able to instrument 8 or more pairs of strips, thus increasing our data-taking rate by an order of magnitude. To that end we developed a year ago a custom preamp board built on the TI LMH5401 8 GHz amplifier, the UFAMP, which was designed to have 900 MHz analog bandwidth and a gain of  $\sim 9$ . We have studied the performance of the UFAMP using a network analyzer and confirmed on the bench with a fast pulser capable of 1 ps risetime edges, and determined that due to parasitic capacitances on the board the actual bandwidth is 300 MHz. Thus, a 2nd revision of the board will need to be produced. While we lost the original designer of the UFAMP (Andrey Sukhanov) to the collider department due to budgetary issues at BNL, we have fortunately added two highly experienced groups, one led by Alexei Denisov of IHEP Protvino, and the other Bruce Kim<sup>13</sup> of CCNY, who is an electrical engineering professor there. They have systematically looked at the impedance of the cathode strip boards and other causes of the reflections noticed in earlier studies. We believe we understand the impedance of the board, which is complicated by the fact that there are multiple connected layers, and that in addition the reflections were exacerbated by a passive summing of the 2 or 3 strips on each channel of readout. The new revision of the preamp board will incorporate the proper impedance matching and actively sum the strips to solve these problems.

Even with the custom preamps, the DRS4 evaluation board limits the number of channels of readout to 4. An 8 channel DRS4 board, which can be run from the same clock to support as many channels of synchronized readout as needed, was designed last year by A. Sukhanov, and improved recently by A. Denisov. A block diagram of the schematic is shown in Fig. 2.5.4. With the rev2 version of the UFAMP preamps and this DRS4 board, we should be able to instrument 8 or more pairs of mRPC strips at a time, and thus vastly increase the speed of studies of the factors affecting mRPC timing performance.

---

<sup>13</sup> <https://www.cuny.cuny.edu/profiles/bruce-kim>

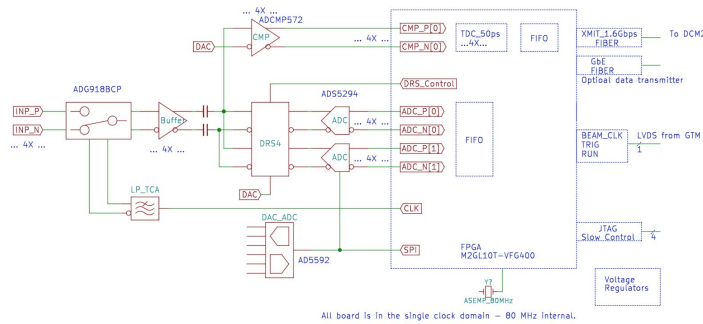


**Figure 2.5.4:** Block diagram for the proposed DRS4-based prototype board.

In addition to the mRPC studies, timing resolution studies of the UV-sensitive MCP-PMT made by ANL will be done. Unfortunately, our plans to use the UV spectrometer in BNL's Instrumentation Dept over the last year have been delayed due to a conflict over its use, since it was needed for studies for the NEXO experiment. We have recently found a UV Spectrometer in the BNL physics dept, and the permission to use it. A summer student will make measurements of the QE from 170-600 nm, the transit time spread (TTS) over that QE range, the TTS as a function of different HV (across different sections of the PMT), and the timing resolution vs number of photoelectrons. The latter is to check if the resolutions scale as it should. Studies of the TTS vs wavelength will help elucidate the mechanism for the surprising increase in QE as one goes down to 170 nm.

A test beam is proposed for the Spring of 2017 to test the variations of mRPCs we will produce, and the TOF MCP-PMT. One major issue during previous test beam runs has been a lack of manpower, so we ask for money to support 1 week of travel for 4 people to go to the FTBF. We also requested funding of \$5K for the production of revision 2 of our custom UFAMP fast preamps, and \$35K for production of the DRS4 digitizer board.

### 2.5.3 TOF R&D Deliverables

#### FY18

- Rev2 of UFAMP (8 GHz preamp) will be developed, built and tested
- Ultra-thin glass (0.1 mm) mRPC will be built and tested in cosmic rays, and in test beam
- DRS4 prototype digitization board will be built and tested
- The QE and the TTS of single photoelectrons of the UV sensitive MCP-PMT will be measured as a function of wavelength down to the cutoff of fused silica at ~170 nm

#### FY19

- Further building and testing of mRPC variants will be done, with the goal of trying to achieve 10 ps resolution
- The UV sensitive MCP-PMT will continue to be tested, with a goal of 5 ps

### 3. Lepton (electron) Identification

Contacts: C. Hyde <[chyde@odu.edu](mailto:chyde@odu.edu)>

The focus of the funded activities of the eRD14 Consortium is on hadron-species identification. However, we have not neglected electron and muon I.D. At an Electron-Ion Collider, detection and identification of the scattered electron is a critical requirement. Many important processes also involve particles decays to leptons (e.g.,  $J/\psi \rightarrow e^+e^-$ ). The baseline system for  $e/\pi$  identification is the electromagnetic calorimeter (EMcal), which is included with  $4\pi$  coverage in all the EIC model detectors. However, the pion suppression achievable in EMcal is limited primarily from charge-exchange events ( $\pi^+p \rightarrow \pi^0n$ ), resulting in an electromagnetic shower indistinguishable from an electron and associated with a charged track. Although different types of EM calorimeters are considered for different parts of the EIC detectors, in general a good EMcal will provide  $e/\pi$  identification up to about 1:100. This can be improved with shape analysis of a high-granularity EM calorimeter, but at the cost of a loss of electron efficiency. Figure 3.1 illustrates the trade-off between PID detection efficiency vs. purity of PID, for a fixed PID separation of two species by  $N\sigma$ . The inclusion of a hadronic calorimeter (HCal) behind the EMcal will only partially improve the  $e/\pi$  identification, since charged pion events that charge-exchange in the EMcal will be mostly contained in the EMcal, and will not give large signals in the HCal. In order to reach kinematics where pion backgrounds are high, additional  $e/\pi$  ID detectors will be needed.

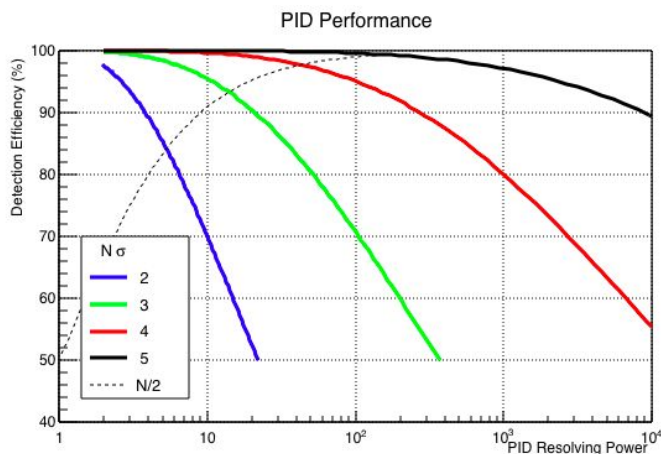


**Figure 3.1:** Contours of constant PID separation,  $N\sigma$ , in the plane of PID efficiency vs. resolving power *vis-a-vis* the unwanted species. The dashed line corresponds to making the PID separation at the midpoint between the two particle-species distributions.

#### 3.1 Electron ID

In the hadron endcap, Fig. 2.1.4 demonstrates  $\geq 3\sigma$   $e/\pi$  separation up to 19 GeV/c by the proposed dual-RICH. For the  $C_2F_6$  gas alone,  $\geq 3\sigma$   $e/\pi$  separation is achieved over the range 5–19 GeV/c. Thus, in the ion endcap, with the dual-RICH together with the EMcal,  $10^3:1$   $e/\pi$  separation is achievable at  $\sim 95\%$  electron efficiency up to 19 GeV.

On the electron endcap side, Fig. 3.2 (left) shows the large background from low-momentum pions. The mRICH (see section 2.3), if implemented in the electron endcap, will provide additional (to the EMcal)  $e/\pi$  discrimination, especially at low momentum, as illustrated in Fig. 3.2 (right). Following the dashed

line of Fig 3.1, the combination of EMcal and mRICH can ensure less than 1% pion contamination in the electron sample over the entire momentum range of Fig. 3.2 (left). We have also proposed (although we do not request funds for FY18) the development of an  $e/\pi$  Cherenkov detector for the electron endcap – a common solution in electron scattering experiments (including CLAS12, SoLID, *etc.*). The technology we would like to pursue for the R&D is a variation of the Hadron Blind Detector (HBD) used at PHENIX, but with the sensors at the endcaps of the cylinder rather than around the barrel.

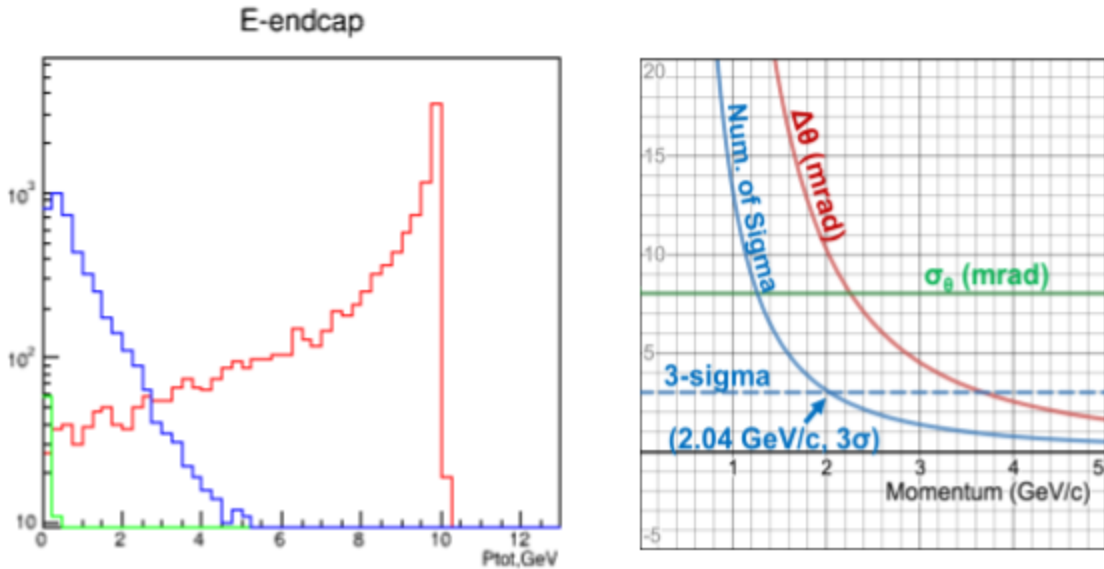


**Figure 3.2** Left: Electron-endcap momentum distributions of scattered electrons (red), negative pions (blue), and secondaries (green) for collisions of 10 GeV electrons on 100 GeV protons (a common BNL / JLab kinematic) from Pythia in a bin of  $1 < Q^2 < 10 \text{ GeV}^2$  for the electrons (pions include photoproduction). Right:  $e/\pi$  discrimination beam-test performance achieved with the mRICH (section 2.3). The green line is the per-photon resolution (mrad). The red line is the  $e-\pi$  separation (mrad). The blue line is the achieved separation in experimental  $\sigma$  of the Cherenkov radii.

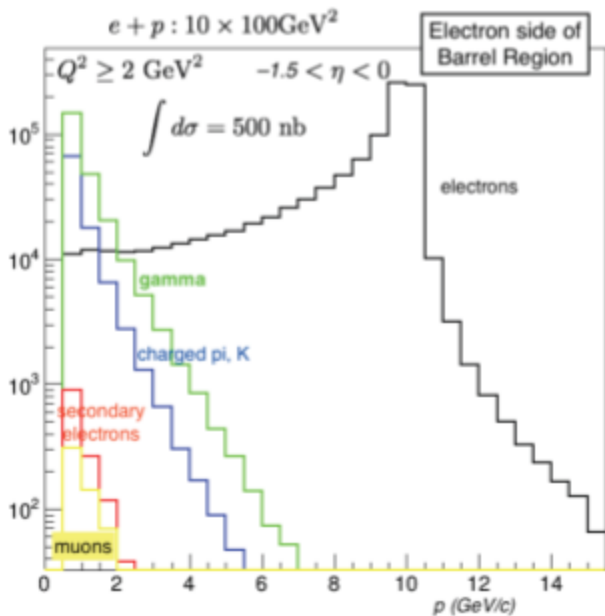


**Figure 3.3:** Central barrel region, negative-pseudorapidity (electron endcap-side), momentum distributions of scattered electrons (black), photons from hadron decays (green), charged  $\pi/K$  (blue), electrons from hadron decays (red) and muons (yellow). Deep Inelastic Scattering events for 10 GeV electrons colliding with 100 GeV/c protons. Events selected for  $Q^2 \geq 2 \text{ GeV}^2$ .

Figure 3.3, similar to Fig. 3.2, shows the particle multiplicities in the negative pseudo-rapidity side (electron-endcap side) of the central barrel region. Below 2 GeV/c,  $e/\pi$  discrimination is again challenging. Figure 2.4.1 outlines the  $e/\pi$  separation achievable with the DIRC. At 2 GeV/c, multiple scattering in the DIRC itself limits the tracking resolution to 1.5 mrad, and this degrades to 2.5 mrad at 1.3 GeV/c. The DIRC will still provide 5:1  $e/\pi$  resolving power over this momentum range, with electron efficiency  $> 85\%$ . This will provide an electron sample with less than 1% pion contamination for all momenta above  $\sim 1.3$  GeV/c.

### 3.2 Muon ID

Muon identification is important for di-lepton production (both inclusive and vector meson decays, *e.g.*  $J/\Psi$ ) and for semi-leptonic decays of heavy flavor hadrons. Every EIC detector concept includes some form of hadron calorimetry in the ion downstream endcap of the central detector. However, the different proposals differ significantly in the central barrel region. We are assessing the BELLE (and its BELLE-I upgrade)  $K_{Long}$  - Muon (KLM) detector as a modest cost option for instrumenting the solenoid return yoke. This has shown good performance for muon ID and modest performance for measuring the energy of high-energy neutrons and K-long mesons.

## 4. Photosensors & Electronics

The specific requirements that the DIRC and the RICH detectors must fulfill within the scope of the EIC pose unique constraints on sensor and electronics performance different from any previous DIRC and/or RICH implementation. Table 1 below lists the minimum requirements on DIRC, mRICH, and dRICH photosensors. Specifically, the small pixel size of 2–3 mm and the immunity to magnetic fields of magnitude in the range 1.5–3 T are unique constraints. The main objective of this R&D effort during the proposed funding period is to identify and assess suitable photosensor and electronics solutions for the readout of the EIC Cherenkov detectors, both for the full EIC detector and for prototypes in beam tests. Depending on the evaluation outcome, design optimization studies of those photosensor and electronics parameters found lacking in the evaluated samples but critical for operations in the EIC environment, will be carried out. In addition to supporting the adaptation of developing photo-sensor technologies for the EIC Cherenkov detectors (such as LAPPDs and GEMs) the goal is to identify a cost-efficient common readout solution that is shared within the EIC-PID consortium. Ultimately, in the long term, this R&D work will allow us to make a recommendation about the best photo-sensors and electronics solutions for the PID detectors in EIC implementation.

### Sensor requirements and options

The consideration of possible photosensor solutions for each detector component is driven by the operational parameters of the detector, with cost optimization in mind. The table below summarizes the performance parameters, which photosensors for the DIRC, mRICH, and dRICH must satisfy.

Parameter	DIRC	mRICH	dRICH
Gain	$\sim 10^6$	$\sim 10^6$	$\sim 10^6$
Timing Resolution	$\leq 100$ ps	$\leq 800$ ps	$\leq 800$ ps
Pixel Size	2–3 mm	$\leq 3$ mm	$\leq 3$ mm
Dark Noise	$\leq 1$ kHz/cm <sup>2</sup>	$\leq 5$ MHz/cm <sup>2</sup>	$\leq 5$ MHz/cm <sup>2</sup>
Radiation Hardness	Yes <sup>14</sup>	Yes <sup>14</sup>	Yes <sup>14</sup>
Single-photon mode operation?	Yes	Yes	Yes
Magnetic-field immunity?	Yes (1.5–3 T)	Yes (1.5–3 T)	Yes (1.5–3 T)
Photon Detection Efficiency	$\geq 20\%$	$\geq 20\%$	$\geq 20\%$

**Table 1** A list of performance requirements for the photosensors for the EIC PID Cherenkov detectors.

Photomultipliers (PMTs) from the currently available pool that are viable candidates for EIC application are Silicon PMTs (SiPMs), Multi-anode PMTs (MaPMTs), commercial Microchannel-Plate PMTs (MCP-PMTs), Large-Area Picosecond Photodetectors (LAPPDs), and Gaseous Electron Multipliers (GEMs).

The key parameters of the photodetectors for the mRICH are small pixel size, resistance to magnetic field, and low cost (due to its large sensor area). Depending on the mRICH location, the requirement for radiation hardness will vary. The detector does not require good PMT timing resolution. GEMs with a photocathode sensitive to visible light, with their good radiation hardness and good position resolution, would be a very good and cost effective solution for the mRICH. SiPMs could be used if their radiation hardness is sufficient. LAPPDs with pixelized readout could be considered as possible photosensors for mRICH detectors if they have resistance to magnetic fields and low cost. MCP-PMTs satisfy the mRICH requirements, however their high cost is a drawback. The key parameter of the photodetectors for the dRICH is the small pixel size. Although the relative sensor area (normalized to the absolute detector area) of this detector is small, due to the large absolute detector area, cost is also an important parameter. Good sensor options for the dRICH would be similar to the ones for mRICH (keeping in mind that due to the location of the sensors, the requirement for radiation hardness is not as important for the dRICH). The key parameters of the photodetectors for a DIRC are fast timing, small pixel size, and a moderate to low dark count rate (DCR). Magnetic-field tolerance is required if the DIRC readout is located within the magnetic field of the solenoid. SiPMs could eventually be possible for DIRC if future developments lower their DCR to an acceptable level. Currently, the only photodetectors satisfying these requirements are MCP-PMTs (including LAPPDs with pixelized readout). Excellent timing resolution ( $\sim 100$  ps) is in particular required for the high-performance DIRC if a time-based PID reconstruction method is adopted for the geometry based on wide radiator plates. Such timing resolution is satisfied by currently commercially available MCP-PMTs, however, development of electronics with good time resolution for small signals may be required.

<sup>14</sup> The EIC radiation levels are expected to be comparable to the levels at current operations of RHIC. The exact level will vary depending on the exact readout location of each PID detector's readout.

## 4.1 Sensors in High-B fields

Contacts: Y. Ilieva <[jordanka@physics.sc.edu](mailto:jordanka@physics.sc.edu)>, C. Zorn <[zorn@jlab.org](mailto:zorn@jlab.org)>

The integration of the three Cherenkov detectors in the central detector involves setting their photo-sensor readouts in the non-uniform fringe field of the solenoid. While an out-of-field readout option for the DIRC may be feasible, an in-field readout is the only option for the two RICH detectors. The objective of this activity, thus, has been to assess the gain and the timing performance of available photosensors in high magnetic fields (due to the maximum field of 5 T attainable by the magnet, we can do the assessment from 0 T up to the field magnitude at which the sensor performance breaks down) and for various relative orientations between the sensor and the magnetic field, and to reasonably support (as needed for the R&D) further design optimization studies of these sensors. The long-term goal of the research is to recommend sensor options for Cherenkov-detectors readout in the magnetic field of the solenoid magnet.

### 4.1.1 FY17 Progress and Achievements

The program for testing photosensors in high magnetic fields was established within eRD4, and has now been taking data for a fourth year. In the past years, the main focus of the activities was the gain evaluation of sensors with different pore sizes. The initial gain studies of single-anode MCP-PMTs with pore size of 3- $\mu\text{m}$  and 6- $\mu\text{m}$  yielded a reasonable performance up to 2 T (although that upper limit depended on the sensor, the applied high voltage, and the orientation of the sensor relative to the field) and showed that overall, sensors with smaller pore size can be operated up to higher magnetic fields. Large gain variations (of about an order of magnitude), depending on the sensor type, with  $(B, \theta, \varphi)$ <sup>15</sup> were also observed. Since the readout of the EIC Cherenkov detectors is considered to be in an area where the solenoid field is non-uniform, finding a way to recover the gain not only at large  $B$ , but also for a large range of relative orientations between the sensor and the B-field is critical. Our gain studies, varying independently the voltages across the three stages: between the photocathode and the MCP ( $V_{C-MCP}$ ), across the two microchannel plates ( $V_{MCP-MCP}$ ), and between the last MCP and the anode ( $V_{MCP-A}$ ), showed that optimizing the voltage across the multi-channel plates can help to recover the gain in B-fields. However, the range of B-field magnitude over which the gain can be fully recovered strongly depends on the angle between the sensor and the field axes. This means that high-voltage optimization alone cannot achieve gain recovery and uniformity over a large range of sensor-field orientations in a field of 3 T.

The results of the single-anode sensor measurements showed that (a) the best multi-anode MCP-PMTs candidates for EIC application are the ones with the smallest pore size and (b) gain measurements varying independently the voltages across the three MCP-PMT stages are important in order to identify the limits of gain optimization and uniformity over a large range of sensor-field orientations by controlling the HV, which is an easily accessible operational parameter.

Currently, the smallest pore size of commercially available multi-anode MCP PMTs is 10  $\mu\text{m}$  and there are two manufacturers that have been producing such sensors, Hamamatsu and Photonis. Photek is in process of developing a small-pore-size multi-anode sensor, which could be of interest for EIC when it becomes available.

---

<sup>15</sup> Here  $\theta$  is the angle between the sensor and the B-field axes and  $\varphi$  is the rotation angle about the sensor axis.

In summer 2016 we evaluated the gain of Hamamatsu (10- $\mu\text{m}$  pore size) multi-anode MCP PMTs as a function of  $(B, \theta)$ . We also did a B-field scan of a 25- $\mu\text{m}$  pore size Planacon sensor at  $\theta=0^\circ$  for systematic purposes. The results are shown in Fig. 4.1.1. The gain of the Hamamatsu sensor increases at small field magnitudes and reaches a maximum at 0.5 T for both test orientations. Above 0.5 T the gain decreases exponentially as the B-field increases, however the decrease is faster at  $10^\circ$  than at  $0^\circ$ . The high voltage on the PMT at which the tests were done was 94% of the maximum recommended value. The voltage across the gap between the two micro-channel plates was 96% of its maximum value, whereas the voltages across the micro-channel plates themselves were 90% of their maximum values. The PMT gain is expected to be affected mostly by a HV increase across these three stages when compensating for the magnetic-field effect. Thus, our measurements were at the limit of the ability to compensate for gain decrease by HV increase.

In Summer 2017 we will map the gain of a 10- $\mu\text{m}$  Planacon as a function of  $(B, \theta, \varphi)$ . This measurement will mostly complete the gain studies of commercially available 10- $\mu\text{m}$  MCP-PMTs. In Spring 2017 ODU procured a pico-second laser to use for time-resolution studies. Design of an optical box compatible with our current test setup is underway.

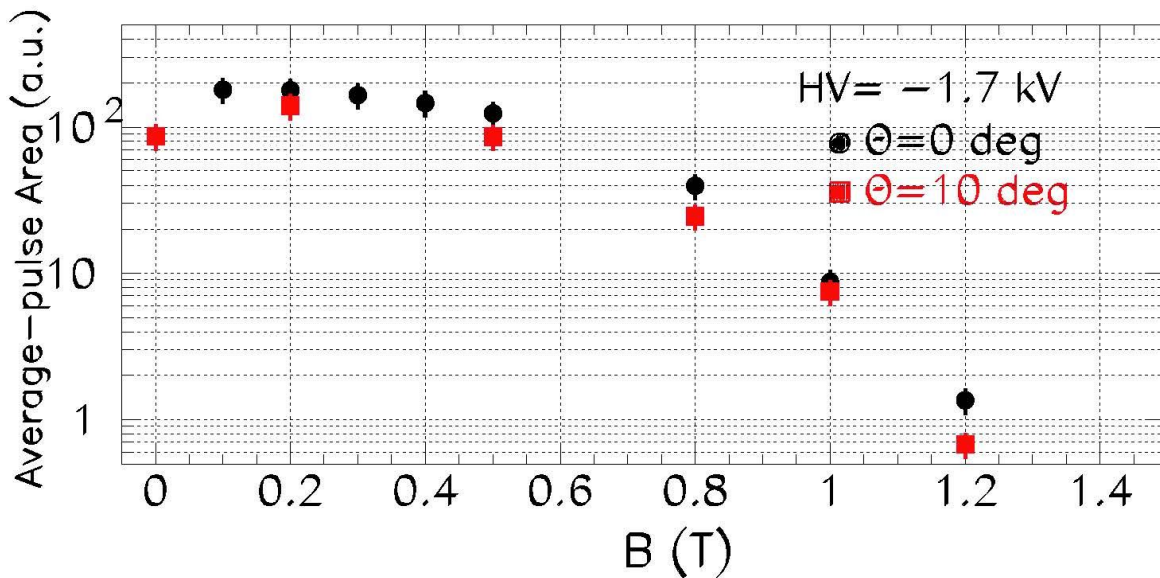


**Figure 3.2.1:** Average-pulse area of Hamamatsu (10- $\mu\text{m}$  pore size) R10754-07-M16 MCP PMT as a function of magnetic-field magnitude.  $\theta$  is the angle between the normal to the PMT front and the B-field vector. Above fields of 0.5 T, the gain at  $\theta=10^\circ$  decreases faster with B than at  $0^\circ$ , which narrows the maximum field at which the sensor can be operated at this orientation. The error bars show preliminary 20% uncertainties dominated by systematics.

In Summer 2017, we started to develop an MCP-PMT simulation. The simulation will be used to study the sensor gain as a function of various design parameters, such as bias angle, ratio of pore-size diameter to channel length, distances between the photocathode and first MCP, between the two MCPs, and the anode and the last MCP, *etc.* Such studies can establish an optimal set of MCP-PMT operational and design parameters, and their limits, for operating the sensors in a range of field magnitudes and orientations similar to what is expected for DIRC and RICH applications in an EIC detector. If a suitable set of design parameters is identified, it will be discussed with MCP-PMT manufacturers in an effort to

produce test samples. Simulations are the most optimal approach for such design optimization as the cost of manufacturing single sensors, each with various geometrical parameters is prohibitive.

#### 4.1.2 Proposed High-B R&D Activities

The main focus for FY18 is to construct and commission the fast laser system, to upgrade the High-B setup with timing electronics, commission the system, and eventually perform first time-resolution evaluation of 10- $\mu\text{m}$  multi-anode sensors in magnetic fields from 0 T up to the maximum field where the gain measurements show that the PMT performance breaks down. The motivation for the timing measurements is given below.

Given the large gain variations with  $(B, \theta, \varphi)$  observed in our measurements during FY14–16, and the solenoid field non-uniformity in the area where the installation of the DIRC<sup>16</sup> readout is considered, it is clear that the gain across the readout will not be uniform. Since the timing resolution of an MCP-PMT depends strongly on the amplitude of the output signal, *i.e.* the sensor's gain, the evolution of the sensors timing response with  $(B, \theta, \varphi, \text{HV})$  needs to be considered. A theoretical model of the electron avalanche development in the MCP suggests that the transit time spread (TTS) of a straight-channel MCP should not depend on the component of the field parallel to the channel axis<sup>17</sup>. No theoretical input exists regarding the effect of transverse fields. Actual timing measurements of chevron-stacked MCPs exist only for magnetic fields up to 2 T. The study done for the development of the BELLE II TOP counter evaluated the timing resolution of a multi-anode Hamamatsu sensor up to 1.5 T for a fixed orientation of the sensor axis relative to the field and found no significant changes<sup>18</sup>. A more comprehensive study was done for the development of the PANDA DIRC as the timing performance was evaluated not only for varying fields but also for varying orientations between the sensor and the field axes<sup>19</sup>. Within the uncertainties of their measurements, the latter study found only a small deterioration of the time resolution towards higher fields. As this study covered a range of fields up to 2 T only, there are no data mapping MCP-PMT timing response above 2 T and it is not known if the observed small deterioration would follow a progressive trend at higher fields. While, based on the published low-field measurements, one expects the timing resolution to deteriorate (if indeed) as the field increases much less than the gain, given the requirement of 100 ps or better timing resolution for the EIC DIRC, it becomes important to evaluate MCP-PMT timing characteristics with  $(B, \theta, \varphi, \text{HV})$ . Naturally, timing measurements will strongly relate to the gain measurements and will also follow up with sensor design optimization as well as with advancements in performance of timing readout electronics. Extending the functionality of the High-B test setup to allow for precise timing measurements is also a natural synergistic activity with the LAPPD project.

Our goal for the future effort of the High-B program is to achieve an MCP-PMT design and operational parameters that are optimized for successful application in the Cherenkov PID detectors in the high magnetic field of the central detector at EIC. This effort will involve (a) High-B timing studies of a variety of commercially available multi-anode MCP-PMTs as a function of various operational

---

<sup>16</sup> DIRC is explicitly mentioned here, since excellent timing resolution is key for the DIRC time-based PID method..

<sup>17</sup> G.W. Fraser, Nucl. Instr. Meth. A **291**, 595 (1990).

<sup>18</sup> S. Hirose, Nucl. Instr. Meth. A **766**, 163 (2014).

<sup>19</sup>A. Lehmann *et al.*, Nucl. Instr. Meth. A **595**, 173 (2008).

parameters, (b) Development and implementation of a simulation of an MCP-PMT in the design process.

#### **FY18 Proposed R&D activities**

- Setup modifications and commissioning for timing studies. The custom laser box for our pico-second laser will be manufactured and commissioned. The dark box holding the measured sensors needs to be also equipped with a safety interlock, which turns the laser off if the box is accidentally opened during measurements. Such a box could be adapted to hold a different laser should the need arise to acquire a faster laser. The laser box will be also used for the LAPPD activities of this R&D. Fast electronics, such as an amplifier and a TDC will be procured. We are cooperating with CAEN to test their new 5-ps resolution TDC samples (which will become available in Summer 2018). We will commission the timing branch of the setup and, if time allows, will perform first time-resolution measurements of 10- $\mu$ m sensors. Due to the decrease of manpower for these activities at JLab in 2018 (due to colleagues moving to new employments), to support the commissioning and the runs at JLab, funding for a second undergraduate USC student is requested for FY18. The funds for the other USC students will be carried over from FY17, when a student had to drop out the internship in early summer and could not be replaced.
- Continuation of the development of MCP-PMT simulation that began in Summer 2017.
- Assessment of the advantages and disadvantages, and eventual negotiation with ANL of a merge of the Jefferson Lab High-B facility with the LAPPD test setup at ANL. Such a merge would capitalize on the existing infrastructures for the LAPPD development at ANL and of the High-B tests at JLab and eventually reduce cost for the R&D program if ANL agrees to support the sensor-test activities from their local LDRD program.

#### **FY19 Proposed R&D Activities**

- Evaluation of timing resolution of multi-anode MCP PMTs, such as 10- $\mu$ m pore-size sensors.
- Commissioning of the SLAC scanning laser system<sup>20</sup> in preparation for sensor tests for detector prototypes (conditional).

The proposed activities of the program are based on our results from the first four program years. As our efforts continue to develop, we will continue to benefit from the expertise of our PANDA GSI collaborators and from the established collaborations with MCP-PMT manufacturers, such as Photech, Photonis, and Hamamatsu as we proceed with the evaluation of their sensors.

#### **4.1.3 High-B R&D Deliverables**

##### **FY18**

- Manufacturing and commissioning of fast-laser optical box.
- Report on multi-anode PMT (Planacon, Hamamatsu) timing resolution as a function of  $(B, \theta, \varphi,$

---

<sup>20</sup> The SLAC laser system delivers a focused laser beam with a scanning capability allowing to move the laser spot along the surface of a sensor. It has been designed for evaluation of MCP PMTs as part of J. Vavra's lab. We have obtained his agreement to potentially move the setup to the High-B facility at JLab. We expect that negotiations between JLab and SLAC to move the equipment, as well as the actual relocation, will happen in FY18. Upon the condition that these are successful, we propose to commission the setup in FY19. The commissioning will primarily involve a software and/or hardware update of the motor control.

HV).

- Progress report on MCP-PMT simulation studies.

## 4.2 LAPPD™ MCP-PMTs

*Contacts: J. Xie <[jxie@anl.gov](mailto:jxie@anl.gov)>, M. Chiu <[chiu@bnl.gov](mailto:chiu@bnl.gov)>*

The LAPPD™ project is a multi-year project involving a number of institutions, with a goal to create an MCP-PMT that has the same very high performance as existing MCP-PMTs, but at a significantly lower cost. Specifically, for the EIC detector R&D, the effort aims to adapt the LAPPDs to the EIC requirements, which include pixelated readout and acceptable performance in high magnetic fields. With these adaptations, the LAPPDs can be used for the readout of mRICH, dRICH, and DIRC detectors, and for TOF applications.

### 4.2.1 FY17 Progress and Achievements

In early FY2017, experimental data obtained in the Fermilab test beam were analyzed to establish the rate capability of MCP-PMTs. The beam tests used the 120 GeV primary proton beam with a beam spot size of about 8 mm<sup>2</sup>. The beam intensity was varied to achieve fluxes from 3.3–150 KHz/cm<sup>2</sup>. Figure 4.2.1 (left) shows the gain dependence on the flux rate. The gain of the tested MCP-PMT is seen to remain approximately constant for rates up to 75 KHz/cm<sup>2</sup>. This rate capability is well sufficient for the EIC requirement.

An attempt to produce MCP-PMT with pixelated readout was carried out in FY2017. We designed a full ceramic base with feed-through pins to bring the signals out from pads that are inside the tube. The design was transferred to Innosys, Inc. to develop a pad-based pixelated readout made with ceramic base and copper pads. Two pixelated readout bases were initially planned for production. However, the company underestimated the technique difficulties of producing such pixelated bases. After a delay of several months, Innosys, Inc. sent us a ceramic pixelated base with several defects as shown in Fig. 4.2.1 (right): the readout pads on the inner side of the anode plate are not flat as requested; the outside connections to these anode pads are not implemented; and the side wall of the tile base is only 3-mm thick, while we specified 5 mm. After being sonicated in water for less than 5 min, three pads (two readout pads and one HV pad) detached from the anode plate, and an open hole showed up under the HV pad that fell off. We have to conclude a failure of producing pixelated readout with ceramic base and copper VIAs. Currently, Innosys, Inc. is still working on overcoming the technique difficulties to provide us with a more reliable pixelated readout. Meanwhile, we have pursued another approach to provide a pixelated readout through capacitive coupling design. The design is to replace the stripline with a resistive anode coated by the ALD method, and to put copper pads for capacitive pickup on the other side of the glass base. Several glass substrates have been coated with the ALD method, providing resistive anode of ~ 10 MΩ. A detector using the resistive anode base is planned to be produced soon.

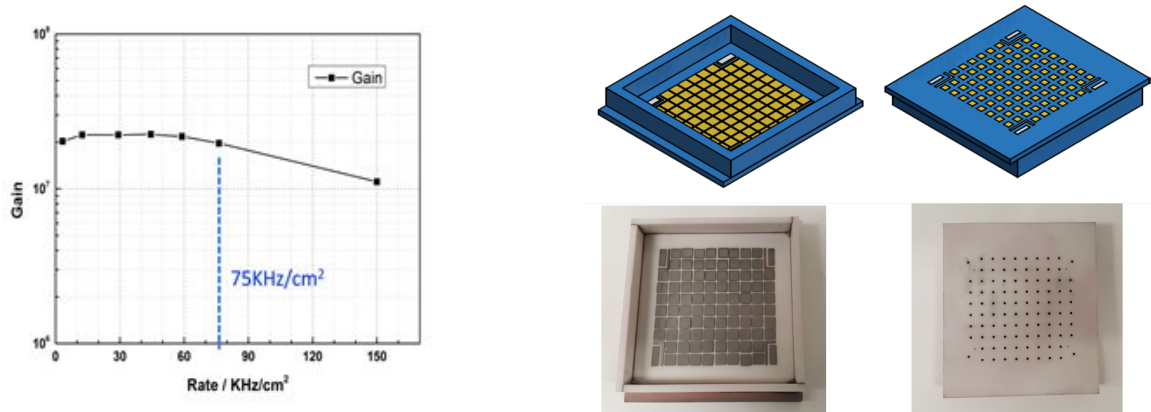


**Figure 4.2.1:** (Left) MCP-PMT gain dependence on flux rate. The rate capability of the tested MCP-PMT is up to 75 KHz/cm<sup>2</sup>, above the EIC requirement. (Right) Design and production of pixelated readout made of full ceramic base and copper VIAs, the as-received base has several defects.

Recently, Argonne acquired a solenoid magnetic-field facility for the calibration of magnetic field probes for the g-2 experiment. As the facility is open for general use, we plan to test MCP-PMT photo-sensors, developed and built at Argonne, at this facility. To this effect we designed and built a transporter and a holder frame for MCP-PMTs with sizes up to 20 x 20 cm<sup>2</sup>. The frame is designed such that the center of the MCP-PMT is aligned with the center of the magnetic field. All components of this holder are made of non-magnetic materials. The transporter can be electronically controlled. The solenoid facility and the transporter are shown in Fig. 4.2.2. In addition to the holder and transporter, a complete MCP-PMT test system was assembled. The system is composed of a 405-nm LED, fiber optics, power supplies, and a CAEN desktop digitizer. The software for operating the system and for data analysis was developed and commissioned. A number of MCP-PMTs with different designs are currently under testing to evaluate their magnetic-field tolerance.



**Figure 4.2.2:** (Left) Schematic of self-designed test stand for MCP-PMT magnetic-field performance testing, up to 20 cm x 20 cm area LAPPDs. (Right) Magnetic field testing of 6 cm x 6 cm MCP-PMT, the MCP-PMT is held in a dark box and ready to be moved into the solenoid magnetic field through a trail.

The commercialization of LAPPD in Incom, Inc. made great progress in FY2017. Several 20 cm x 20 cm LAPPDs have been successfully produced for early user testing and characterization. ANL is expected to receive a 20 cm x 20 cm LAPPD in early FY18 for full characterization and especially for magnetic-field performance testing.

#### 4.2.2 Proposed LAPPD R&D Activities

##### FY18

- Produce pixelated readout board with 2.5 mm x 2.5 mm pad size.
- Test the MCP-PMT with capacitive coupling pixelated readout.
- Produce a detector with 10- $\mu$ m pore size MCP and reduced spacing, for fast timing ( $<10$  ps) and improved magnetic-field performance specifically for EIC applications.
- Test the performance of 10- $\mu$ m pore size MCP-PMT.
- Modify ANL characterization facility to suit for the 20 cm x 20 cm LAPPD characterization.
- Evaluate the performance of 20 cm x 20 cm LAPPD for EIC application.

##### FY19

- Finalize testing of the pixelated readout in test beam at Fermilab.
- Finish testing of the Incom LAPPD in test beam at Fermilab.
- Publish papers on the test results of MCP-PMTs.

#### 4.2.3 LAPPD R&D Deliverables

##### FY18

- MCP-PMT with variable pixelated readout.
- MCP-PMT with better capabilities for fast timing and magnetic field tolerance.

##### FY19 (tentative)

- Finalize testing of LAPPDs and MCP-PMTs.
- Publish papers on experimental results.

### 4.3 Readout Sensors and Electronics for Detector Prototypes

*Contacts: G. Varner <[varner@phys.hawaii.edu](mailto:varner@phys.hawaii.edu)>, M. Contalbrigo <[mcontalb@fe.infn.it](mailto:mcontalb@fe.infn.it)>*

The development of advanced, high-performance RICH and DIRC detectors poses new demands on photosensors and requires new readout electronics. All eRD14 Cherenkov systems envision using small pixels (2-3 mm), while the DIRC also needs to obtain good timing ( $< 100$  ps) with the relatively small pulses produced by MCP-PMTs. While initial prototype tests have been made with larger pixels and poorer timing to validate Monte Carlo simulations which were then used to infer the performance of the systems developed for the EIC, future prototypes will have to be able to directly demonstrate the desired PID performance. To achieve this, new readout electronics have to be developed. In addition, while a demonstration of the PID performance can be achieved using simpler sensors (*e.g.*, MaPMTs for the two RICH detector prototypes), the final EIC application will impose additional constraints, such as operation

in the magnetic field of the solenoid as well as a minimization of the total system cost. Thus, it is also important to be able to test alternative sensors, such as SiPMs for the RICH detectors.

To address the slightly different requirements and timelines of the various systems, we have developed a common consortium-wide strategy that provides a complete solution while maximizing synergies and minimizing cost. The Hawaii group will take the main responsibility for the development of the front-end electronics (ASICs and boards) while INFN will have the lead on integration for both the sensors and back-end / DAQ. The development has been staged, from almost ready-to-go systems to provide a reliable reference based on a consolidated technology to innovative solutions optimized for the EIC prototypes. For the front end, the older Maroc-based system that was used in the first mRICH test beam (and is also used for CLAS12) will be adapted for sensors (MaPMTs, SiPMs) with smaller pixels. This will provide a fallback solution, and allow to explore different cooling options for the SiPMs. A new front end will also be developed based on the TARGETX chip, which will be integrated on a board directly matching the footprint of the sensors. In contrast to Maroc, TARGETX can also provide the high-resolution timing required by high-performance DIRC detectors using time-based reconstruction algorithms. Ultimately, TARGETX would be replaced by the lower-power, higher-performance SiREAD chip, which is currently in development (with SBIR I funding), but EIC experience with TARGETX would facilitate proper integration of the new chip. The SiREAD effort will also benefit from work the ASoC (System-on-Chip), which has now received SBIR II funding. We hope that SiREAD will be available for instrumenting the PANDA DIRC prototype with small-pixel MCP-PMTs once the prototype is moved to the US in FY19 specifically for the EIC R&D effort after the PANDA R&D is completed. For the back end we plan to use initially a scalable evolution of the system used in the first mRICH beam test, followed by an adaptation of the data acquisition (DAQ) now in development for CLAS12. The latter will be integrated with all three front ends and be able to collect data from multiple sensors. Incorporating a larger volume for the readout, the new mRICH prototype will also serve as a prototype for the development of the readout electronics. After the completion of the Fermilab beam tests, the integration with the JLab DAQ will make it possible to, at least in principle, use the mRICH for further parasitic tests at JLab of both the detector and TARGETX / SiREAD- based readout.

The use of sensors with a small pixel size (2–3 mm) should allow to validate the PID performance of the mRICH, dRICH, and high-performance DIRC prototypes. The H13700-03 MaPMTs acquired in FY17 by GSU provide the baseline solution for testing the optics of the RICH prototypes, a goal for which tolerance to magnetic fields is not required. SiPMs represent an innovative solution with several advantages potentially interesting for EIC (such as robustness, low bias voltage, cost-effective industrial production, magnetic-field compatibility, low material budget), but also some limitations (high noise, low radiation hardness). For the DIRC, MCP-PMTs with a similar footprint will be required to provide the desired timing performance. This is also the type of sensor that would be used in a final DIRC application.

In FY18, the proposed activity aims to provide a reliable readout system for the dRICH and mRICH prototypes by adapting the CLAS front-end electronics to sensors of small pixel size. The back-end, initially based on a generic TCP/IP protocol, will eventually be migrated to the SSP protocol developed

for CLAS DAQ. The new protocol offer a scalable solution compatible with the various front-end chips. The development of a custom solution for SiPM matrices integrating a cooling system will be initiated.

The electronics developed for CLAS12 has been designed to readout MaPMTs and to be compatible with SiPMs. The version working with an optical link and a TCP/IP protocol is suitable for a prototype as it is compact, offers simultaneous digital and analog readout, and flexible trigger conditions (external, auto and self). In order to match it to the H13700 sensors, an adapter board distributing the 256 channels (16x16) over two readout units and an updated DAQ scheme to run several readout units simultaneously would be needed. INFN has several SiPM matrices of various sizes and, in particular, 3 large 16x16 MPPC matrices which are comparable to the H13700 pixel geometry, see Fig. 4.3.1. The large matrices are BGA mounting and should be mounted on a dedicated PCB supporting a cooling system for temperature control. The INFN groups have already experience in studying the performance of SiPM in the single-photon regime for Cherenkov applications. Promising results were obtained but additional work is needed to prove a realistic working condition in single-photon mode, taking into account the high dark count rate and the performance degradation resulting from irradiation. The funding request cover the costs of the CLAS12 front-end electronic adaptation to the small pixel sensors.

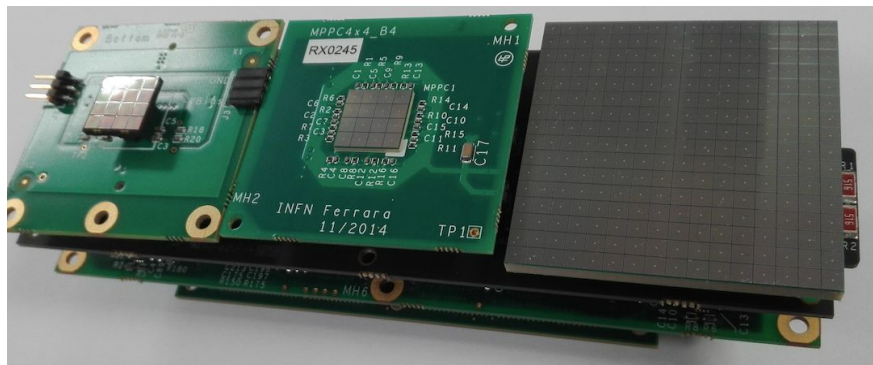


**Figure 4.3.1:** SiPM matrices under test with the RICH electronics.

Highly integrated, low-power, and high-performance readout of 256-anode, 50-mm photosensors is being studied at the University of Hawaii, which has extensive experience in developing electronics for modern PID systems, such as the Belle II TOP DIRC. The proposed system can be adapted to read out all the photosensors (MaPMT, MCP-PMT, SiPM) that are being considered for the various RICH and DIRC detector prototypes being developed by the EIC PID consortium. A compact board stack mates in the envelope directly behind the photosensors, permitting seamlessly abutting together an array of such devices. Each board stack consists of an interface board, which mates directly to the photodetector high-density signal connectors and hosts the waveform sampling ASICs, as well as a digital interface node. A simple and standard power and serial interface allows groups of these 256-anode devices to be collected into a single ethernet acquisition node. The first version of this readout will use a TARGET family ASIC, which has been successfully deployed in 10's of thousands of channel quantities for applications such as large muon systems or atmospheric gamma Cherenkov camera readout. Pairs of these 16-channel ASICs are mounted onto tiny DIMM cards, mounted onto the interface board. As a second phase, reduced power and further compactness will be realized by upgrading to the 64-channel SiREAD

ASIC, when it becomes available. Both the TARGET and SiREAD ASICs are developed by the Hawaii group. The high-speed sampling used by both chips provide the timing resolution required for the DIRC, and can provide readout of waveforms during test beam conditions, which can be helpful for interpreting the data. Funding is requested for \$20k of graduate student time to complete layout of the 3 boards, coordinate their assembly, verify functionality of first prototypes, and characterize their performance. Fabrication and population of these first prototypes is estimated as \$10k, including printed circuit board and component costs.

The proposed back end and DAQ based on the SSP protocol would be compatible with both the current CLAS12 (Maroc-based) front end electronics, and the new (TARGETX, SiREAD) electronics developed by U. Hawaii. It would be developed by the INFN group in collaboration with the JLab DAQ and fast electronics groups.

#### **4.3.1 Proposed R&D Activities**

##### **FY18**

- Development of readout electronics for mRICH and dRICH prototypes compatible with sensors of small pixel size.
- Adaptation of the readout for the use of SiPM arrays.

##### **FY19**

- Development of a readout using SiPM arrays with realistic cooling and scalable readout electronics.
- Characterization of performance and validation of cost for compact and lower power readout variant using the SiREAD ASIC.

#### **4.3.2 Proposed R&D Deliverables**

##### **FY18**

- Initial readout system based upon current CLAS12 readout
- 4x 256 anode photosensor readout for beam test and other evaluation based upon the TARGETX ASIC

##### **FY19 (tentative)**

- Second generation firmware and improved data throughput for front-end to back-end communications
- Integrated system to readout SiPM with temperature control
- Modular and scalable 256-channel building block readout based on the SiREAD ASIC.

## **5. Budget**

### **5.1 Budget Request**

As our baseline (100% level), we request \$420k for FY18, but also provide budgets reduced by 20% and 40%, labelled “80%” and “60%” in the tables below. We also provide guidance on our plans for FY19 in each section above, but do not include summaries for all FY19 options in this section. However, please

note that in some cases items which would not be funded in the reduced-budget scenarios would be shifted into FY19. Also, please note that the “80%” level budget is somewhat lower than the \$329k awarded for eRD14 in FY16, while the “60%” level is close to the \$244k awarded after the large cuts in FY17. The “100%” level is lower than the requests in both FY16 and FY17. All budget items include overhead at the receiving institution. Breakdown of the request by project and institution can be found below for all three funding levels. The consortium funds have been distributed among participating institutions so as to minimize overhead and maximize flexibility. The SOWs will be submitted with wording reflecting the possibility for institutions to fund collaborators at other institutions, for instance to cover travel costs.

### 5.2 Dual-Radiator RICH (dRICH)

	<u>100%</u>	<u>80%</u>	<u>60%</u>
Postdoc, INFN/USC, 8 months (Alessio Deldotto)	\$31.5k	\$31.5k	\$31.5k
Prototype	\$5k	\$5k	
<i>Total</i>	<b>\$36.5k</b>	<b>\$36.5k</b>	<b>\$31.5k</b>

### 5.3 Modular Aerogel RICH (mRICH)

	<u>100%</u>	<u>80%</u>	<u>60%</u>
Postdoc, INFN, 6 months (Luca Barion)	\$22.5k	\$22.5k	\$22.5k
Grad student, GSU (Cheuk-Ping Wong)	\$33.2k	\$30.2k	\$25.7k
Grad student, GSU (new hire in FY18)	\$15.1k	\$12.1k	\$7.6k
Materials, GSU	\$3k	\$1.5k	
Aerogel, INFN	\$5k		
Travel and Conference fee, INFN/GSU	\$21k	\$15.5k	\$9k
<i>Total</i>	<b>\$99.8k</b>	<b>\$81.8k</b>	<b>\$64.8k</b>

### 5.4 DIRC

	<u>100%</u>	<u>80%</u>	<u>60%</u>
Postdoc, CUA, 50% (hired in Q4 FY17)	\$50k	\$50k	\$50k
Undergraduate summer student, CUA	\$5k	\$5k	
Optical samples for tests of radiation hardness	\$5k	\$5k	\$5k
PHOTONIS Planacon XP85122-S MCP-PMT	\$16k		
Travel, CUA/GSI	\$18k	\$15k	\$12k
<i>Total</i>	<b>\$94k</b>	<b>\$75k</b>	<b>\$67k</b>

### 5.5 TOF

	<u>100%</u>	<u>80%</u>	<u>60%</u>
Preamplifier and DRS4 Electronics Production	\$35k	\$20k	\$5k
Travel	\$8k	\$6.5k	\$6.5k
<i>Total</i>	<b>\$43k</b>	<b>\$26.5k</b>	<b>\$11.5k</b>

### 5.6 Sensors in High-B Fields

	<u>100%</u>	<u>80%</u>	<u>60%</u>
LHe and materials for high-B run, JLab	\$10.5k	\$10.5k	\$10.5k
Undergraduate student, USC	\$7.7k	\$7.7k	
Travel, USC	\$9.5k	\$9.5k	\$12k
<i>Total</i>	<b>\$27.7k</b>	<b>\$27.7k</b>	<b>\$22.5k</b>

### 5.7 LAPPDs

	<u>100%</u>	<u>80%</u>	<u>60%</u>
Labor	\$60k	\$40k	\$40k
Materials	\$15k	\$10k	\$5k
<i>Total</i>	<b>\$75k</b>	<b>\$50k</b>	<b>\$40k</b>

### 5.8 Readout Sensors and Electronics for Detector Prototypes

	<u>100%</u>	<u>80%</u>	<u>60%</u>
Front-end readout electronics, Hawaii	\$30k	\$30k	\$25k
Readout adaptation H13700, INFN	\$4k	\$4k	\$4k
Readout adaptation SiPMs, INFN	\$8k	\$4k	
<i>Total</i>	<b>\$44k</b>	<b>\$38k</b>	<b>\$29k</b>

### 5.9 Budget by project

	<u>100%</u>	<u>80%</u>	<u>60%</u>
dRICH	\$36.5k	\$36.5k	\$31.5k
mRICH	\$99.8k	\$81.8k	\$64.8k
DIRC	\$94k	\$75k	\$67k
TOF	\$43k	\$26.5k	\$11.5k
high-B	\$27.7k	\$27.7k	\$22.5k
LAPPD	\$75k	\$50k	\$40k
Electronics	\$44k	\$38k	\$29k
<i>Total</i>	<b>\$420k</b>	<b>\$335.5k</b>	<b>\$266.3k</b>

### 5.10 Budget by institution

	<u>100%</u>	<u>80%</u>	<u>60%</u>
ANL	\$75k	\$50k	\$40k
BNL	\$38k	\$21.5k	\$6.5k
CCNY	\$5K	\$5K	\$5K
CUA (and GSI)	\$94k	\$75k	\$67k
GSU	\$66.3k	\$53.3k	\$42.3k
U. Hawaii	\$30k	\$30k	\$25k
INFN	\$52.5k	\$41.5k	\$26.5k
JLab	\$10.5k	\$10.5k	\$10.5k
USC (and INFN)	\$48.7k	\$48.7k	\$43.5k
<i>Total</i>	<b>\$420k</b>	<b>\$335.5k</b>	<b>\$266.3k</b>

## Appendices

### Appendix A

#### List of R&D Publications and Presentations

##### 2017 -- Publications

1. A. Del Dotto, C.-P. Wong *et al.* (EIC PID Consortium), *Design and R&D of RICH detectors for EIC experiments*, NIM A <https://doi.org/10.1016/j.nima.2017.03.032>
2. J. Wang *et al.*, *Design improvement and bias voltage optimization of glass-body microchannel plate picosecond photodetector*, Nuclear Science IEEE Transactions (in print) 2017.
3. C.P. Wong *et al.*, *Modular focusing ring imaging Cherenkov detector for Electron-Ion Collider experiments*, submitted to NIM A, 2017.

##### 2017 -- Presentations

1. R. Dzhygadlo for the EIC DIRC Collaboration, *DIRC-based PID for the EIC Central Detector*, oral presentation at the DPG spring meeting, Muenster, March 27-31, 2017.
2. X. He for the EIC PID Consortium, *Ring Imaging Cherenkov Detector Technologies for Particle Identification in the Electron-Ion Collider Experiments*, has been accepted as a parallel talk at PANIC2017, in Beijing, September 1 - 5, 2017.

##### 2016 -- Publications

1. Y. Ilieva *et al.*, *MCP-PMT Studies at the High-B Test Facility at Jefferson Lab*, JINST **11**, 2016; <http://dx.doi.org/10.1088/1748-0221/11/03/C03061>. Proceedings of the International Workshop on Fast Cherenkov Detectors - Photon detection, DIRC design and DAQ, November 11–13, 2015, Giessen, Germany.
2. G. Kalicy *et al.*, *High-performance DIRC detector for Electron Ion Collider*, submitted to JINST, 2016; Proceedings of the International Workshop on Fast Cherenkov Detectors - Photon detection, DIRC design and DAQ, November 11–13, 2015, Giessen, Germany.
3. J. Xie *et al.*, *Development of a low-cost fast-timing microchannel plate photodetector*, Nucl. Instrum. Meth. A 824 (2016) 159-161.
4. L. Allison: *High-performance DIRC detector for use in an Electron-Ion Collider*, Proceedings for ICHEP2016 (38th International Conference on High Energy Physics), August 3-10, 2016, Chicago, IL, submitted to Proceedings of Science.

##### 2016 -- Presentations

1. H. Hamilton, *Testing of Advanced Particle Detectors for the Next Generation Particle Collider*, oral presentation at the Abilene Christian University Undergraduate Research Festival, 5 April 2016, Abilene, TX.
2. C. Towell, *Development of an Electron Ion Collider Detector Test Stand*, oral presentation at the Abilene Christian University Undergraduate Research Festival, 5 April 2016, Abilene, TX.

3. A. Del Dotto for the EIC PID consortium, *Design and R&D of RICH detectors for EIC experiments*, poster presented at RICH 2016, 9th International Workshop on Ring Imaging Cherenkov Detectors, Slovenia on September 5-9, 2016.
4. Z.W. Zhao for the EIC PID consortium, EIC RICH R&D, presentation at EIC User Group Meeting, January 2016.
5. L. Allison for the EIC DIRC Collaboration, *Particle ID with DIRC Detectors*, invited talk at ODU Nuclear Group Seminar, March 17, 2016.
6. G. Kalicy for the EIC DIRC Collaboration, *DIRCs*, invited talk at ODU Nuclear Group Seminar, December 4, 2016.
7. G. Kalicy for the EIC DIRC Collaboration, *DIRC@EIC*, presentation at EIC User Group Meeting, January 2016.
8. G. Kalicy: PID systems for the JLab EIC full-acceptance detector, ICHEP2016 38th International Conference on High Energy Physics, August 3–10, 2016, Chicago, IL.
9. J. Xie *et al.*, *Planar microchannel plate photomultiplier with VUV-UV-Vis full range response for fast timing and imaging applications*, accepted for RICH 2016, 9th International Workshop on Ring Imaging Cherenkov Detectors, Slovenia on September 5-9, 2016.
10. C.P. Wong, *Performance Study of a Prototype Modular RICH Detector for EIC Experiments*, oral presentation at 2016 Fall Meeting of the APS Division of Nuclear Physics, October 13–16, 2016, Vancouver, Canada.

#### 2015 -- Publications

1. J. Wang *et al.*, *Development and testing of cost-effective, 6cm × 6cm MCP-based photodetectors for fast timing applications*, Nucl. Instrum. Meth. A 804 (2015) 84–93.

#### 2015 -- Presentations

1. H. Hamilton, *Improved Timing Instruments for Particle Identification*, oral presentation at the Abilene Christian University Undergraduate Research Festival, March 31, 2015, Abilene, TX.
2. C. Towell, *Building Detectors to Study a New Phase of Matter*, oral presentation at the Abilene Christian University Undergraduate Research Festival, March 31, 2015, Abilene, TX.
3. E. Bringley *et al.*, *Experimental Setup and Commissioning of a Test Facility for Gain Evaluation of Microchannel-Plate Photomultipliers in High Magnetic Field at Jefferson Lab*, poster presentation at the University of South Carolina Discovery Day, 24 April 2015, Columbia, SC.
4. C. Barber, *Gain Evaluation of Micro-Channel-Plate Photomultipliers in the Upgraded High-B Test Facility at Jefferson Lab*, poster presentation at the Conference Experience for Undergraduates at the 2015 Fall Meeting of the APS Division of Nuclear Physics, October 28–31, 2015, Santa Fe, NM; BAPS.2015.DNP.EA.37.
5. H. Hamilton, *Testing of multigap Resistive Plate Chambers for Electron Ion Collider Detector Development*, poster presentation at the Conference Experience for Undergraduates at the 2015 Fall Meeting of the APS Division of Nuclear Physics, October 28–31, 2015, Santa Fe, NM; BAPS.2015.DNP.EA.9.
6. C. Towell, *Cosmic Test Stand Development for Electron Ion Collider Detector R&D*, poster presentation at the Conference Experience for Undergraduates at the 2015 Fall Meeting of the APS Division of Nuclear Physics, October 28–31, 2015, Santa Fe, NM; BAPS.2015.DNP.EA.20.

7. Y. Ilieva for the EIC DIRC Collaboration, *MCP-PMT Studies at the High-B Test Facility at Jefferson Lab*, invited talk at the International Workshop on Fast Cherenkov Detectors - Photon detection, DIRC design and DAQ, November 11–13, 2015, Giessen, Germany.
8. G. Kalicy for the EIC DIRC Collaboration, *High-performance DIRC detector for Electron Ion Collider*, invited talk at the International Workshop on Fast Cherenkov Detectors - Photon detection, DIRC design and DAQ, November 11–13, 2015, Giessen, Germany.
9. L. Allison for the EIC DIRC Collaboration, *Studies of prototype 3-component lens in CERN test beam and on a test bench at ODU*, invited talk at the International Workshop on Fast Cherenkov Detectors - Photon detection, DIRC design and DAQ, November 11–13, 2015, Giessen, Germany.
10. G. Kalicy for the EIC DIRC Collaboration, *DIRC detectors*, presentation at JLab seminar, Newport News, December 2015.
11. G. Kalicy for the EIC DIRC Collaboration, *Photosensors tests at high B facility in JLab*, presentation at meeting with Photonis in Lancaster, PA, October 2015.
12. G. Kalicy for the EIC DIRC Collaboration, *Photosensors tests at high B facility in JLab*, presentation on meeting with Hamamatsu at JLab, September 2015.
13. G. Kalicy for the EIC DIRC Collaboration, *Developing DIRC Technology*, presentation at ODU Colloquium, Norfolk VA, April 2015.
14. R. Dzhygadlo for the EIC DIRC Collaboration, *DIRC-based PID for the EIC Central Detector*, oral presentation at the DPG spring meeting, Heidelberg, March 23–27, 2015.
15. C.P. Wong, *Simulation Study of RICH Detector for Particle Identification in Forward Region at Electron-Ion Collider*, oral presentation at APS April Meeting 2015, April 11–14, 2015, Baltimore, MD.

#### **Prior 2015 -- Presentations**

1. C. Nickle, *Experimental Setup for Magnetic-Field Tests of Small-Size Light Sensors at Jefferson Lab*, poster presentation at the Conference Experience for Undergraduates at the 2013 Fall Meeting of the APS Division of Nuclear Physics, October 23–26, 2013, Newport News, VA; BAPS.2013.DNP.EA.121.
2. E. Bringley *et al.*, *Experimental Setup and Commissioning of a Test Facility for Gain Evaluation of Microchannel-Plate Photomultipliers in High Magnetic Field at Jefferson Lab*, poster presentation at the Conference Experience for Undergraduates at the 4th Joint Meeting of the APS Division of Nuclear Physics and the Physical Society of Japan, October 7–11, 2014, Waikoloa, Hawaii; BAPS.2014.HAW.GB.140.
3. H. Hamilton, *Time of Flight Detector Development for Future Heavy Ion Experiments*, poster presentation at the Conference Experience for Undergraduates at the 4th Joint Meeting of the APS Division of Nuclear Physics and the Physical Society of Japan, October 7–11, 2014, Waikoloa, Hawaii; BAPS.2014.HAW.GB.149.
4. C. Towell, *Developing a High Precision Cosmic Test Stand for PHENIX Research and Development*, poster presentation at the Conference Experience for Undergraduates at the 4th Joint Meeting of the APS Division of Nuclear Physics and the Physical Society of Japan, October 7–11, 2014, Waikoloa, Hawaii; BAPS.2014.HAW.GB.147.